ADVANCED ENERGY MATERIALS
www.advenergymat.de

Opportunities of Aqueous Manganese-Based Batteries with Deposition and Stripping Chemistry

Mingming Wang, Xinhua Zheng, Xiang Zhang, Dongliang Chao, Shi-Zhang Qiao, Husam N. Alshareef, Yi Cui, and Wei Chen**

Rechargeable aqueous manganese-based batteries have been attracting significant attention owing to their advantages of low cost, high safety, and ease of manufacturing, which are promising attributes for grid-scale energy storage applications. However, most traditional manganese-based batteries with solid-state conversion and intercalation reactions suffer from low capacity and poor long-term cycling stability. The recent novel storage mechanism based on cathode Mn^{2+}/MnO_2 deposition/stripping chemistry has fundamentally tackled these issues, enabling a new generation of manganese-based batteries with superior electrochemical performance. Here, the recent advances in aqueous manganese-based batteries with the Mn^{2+}/MnO_2 deposition/stripping chemistry are reviewed. A summary of the development of manganese-based batteries with different storage mechanisms is provided and new opportunities for the emerging Mn^{2+}/MnO_2 chemistry in the latest generation are highlighted. Then, the current understanding of the Mn^{2+}/MnO_2 charge storage mechanism and its potential in manganese-based batteries for large-scale energy storage applications is presented. Moreover, insights into opportunities and future directions for manganese-based batteries with the Mn^{2+}/MnO_2 chemistry are proposed.

1. Introduction

In order to alleviate the drastic impact of fossil fuels on climate change, environmental pollution, and quality of life, there has never been a greater and more urgent demand of sustainable energy.[1–4] The intermittency of the renewable energy resources such as solar and wind calls for the development of low-cost and scalable energy storage technologies.[5–10] Rechargeable batteries[11–19] are regarded as the most efficient energy storage technologies that have been widely applied to portable electronics, electric vehicles and grid-scale energy storage. Although lithium ion batteries are dominating the current market of electric vehicles and portable electronic devices,[20–24] their application in grid-scale energy storage is just beginning due to relatively high cost, limited service life, and safety concerns.[25–30] Other existing rechargeable batteries such as sodium-sulfur (Na-S), lead-acid, and redox-flow batteries have been gradually applied to the grid storage, but they have encountered different obstacles that need to be overcome, as summarized in **Figure 1**. For example, the Na-S batteries have potentially severe safety issue due to their operation at high temperature (≈350 °C). The lead-acid batteries exhibited poor cycling stability (typically less than 1000 cycles). The redox-flow batteries demonstrated relatively low energy density and high cost in system level. By contrast, aqueous rechargeable batteries offer an alternative energy storage technology for grid storage due to their ease of fabrication, fast operation rates, and good safety.[31–37] Among them, aqueous manganese (Mn)-based batteries have been attracting much research and industry interests owing to their additional advantages of low cost,[38,39]

M. Wang
Department of Chemistry
School of Chemistry and Materials Science
University of Science and Technology of China
Hefei, Anhui 230026, China

X. Zheng, X. Zhang, Prof. W. Chen
Department of Applied Chemistry
School of Chemistry and Materials Science
University of Science and Technology of China
Hefei, Anhui 230026, China
E-mail: weichen1@ustc.edu.cn

Dr. D. Chao, Prof. S.-Z. Qiao
School of Chemical Engineering & Advanced Materials
The University of Adelaide
Adelaide, South Australia 5005, Australia

The ORCID identification number(s) for the author(s) of this article can be found under https://doi.org/10.1002/aenm.202002904.

DOI: 10.1002/aenm.202002904

Prof. H. N. Alshareef
Materials Science and Engineering
King Abdullah University of Science and Technology (KAUST)
Thuwal 23955-6900, Saudi Arabia

Prof. Y. Cui
Department of Materials Science and Engineering
Stanford University
Stanford, CA 94305, USA
E-mail: yicui@stanford.edu

Prof. Y. Cui
Stanford Institute for Materials and Energy Sciences
SLAC National Accelerator Laboratory
Menlo Park, CA 94025, USA

Prof. W. Chen
Division of Nanocatalysis and Energy Conversion
Hefei National Laboratory for Physical Sciences at the Microscale
University of Science and Technology of China
Hefei, Anhui 230026, China

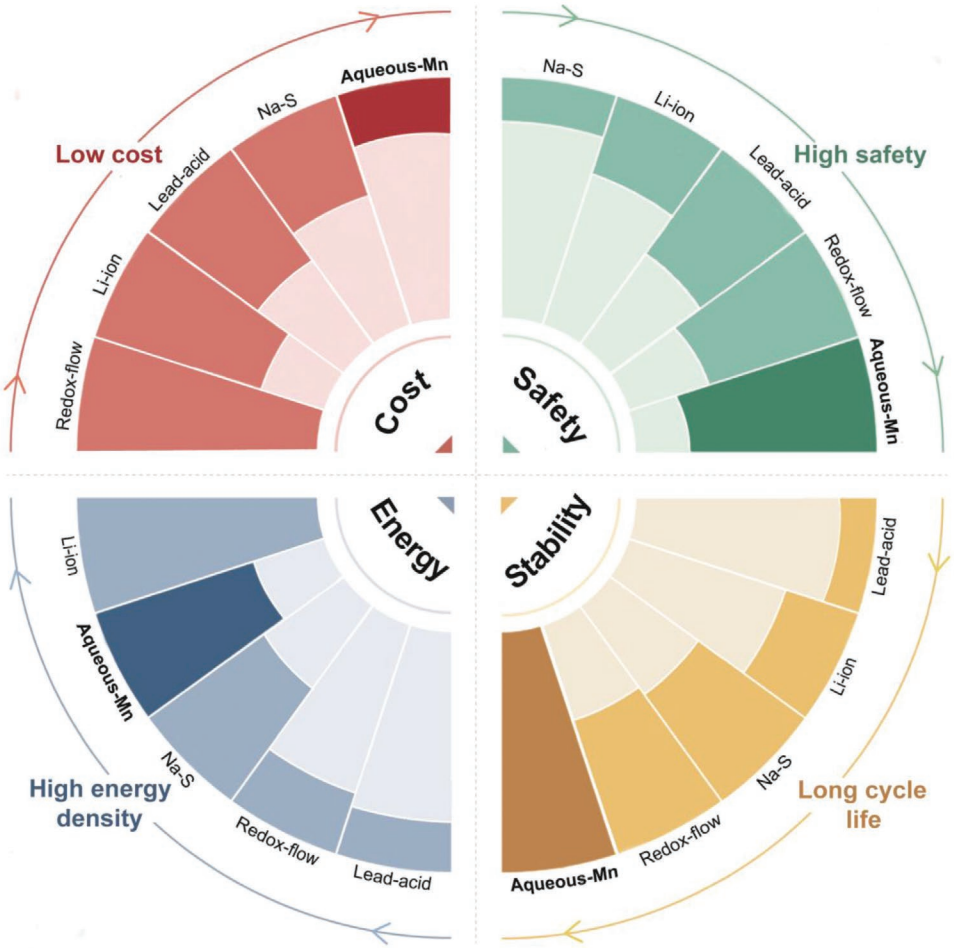

Figure 1. A comparison of aqueous Mn-based batteries with other battery technologies of Li-ion, Na-S, lead-acid, and redox-flow batteries in terms of cost, safety, stability, and energy density for grid-scale energy storage. All data are comparative but not absolute values based on literature.

environmental friendliness,[40] high theoretical capacity, and energy density (Figure 1).[41,42] Moreover, they offer rich redox chemistry thanks to the existence of various valence states such as Mn^0, Mn^{2+}, Mn^{3+}, Mn^{4+}, Mn^{6+}, and Mn^{7+}.[33,43–50] Due to the relatively high electrochemical potentials between Mn^{2+}, Mn^{3+}, and Mn^{4+}, which are the most commonly available valences of the Mn element,[51–53] the Mn-based electrodes in different forms of oxides and hydroxides (e.g. $Mn(OH)_2$, MnOOH, Mn_2O_3, and MnO_2) are typically utilized as cathodes in the rechargeable aqueous batteries.[54–56]

Historically, the MnO_2 cathodes have been studied extensively for the Mn-based aqueous batteries.[57–60] Dating back to the early 1860s, Georges Leclanché[61] invented the first primary MnO_2-Zn cell on the basis of MnO_2-carbon black cathode, Zn foil anode, and a mixture of $ZnCl_2$ and NH_4Cl electrolyte. Thereafter, the studies of MnO_2 and its composite materials in different rechargeable batteries have been increased exponentially.[62–71] Much effort has been devoted to the improvement of electrochemical performance of the aqueous Mn-based batteries. Despite significant progress achieved over the past decades, the Mn-based batteries still encountered fundamental issues that severely hindered their practical applications, such as low capacity, slow charge/discharge rate, and poor electrochemical stability.[72–75] The past attempts on the exploration of Mn-based batteries were based on storage mechanisms of solid-state conversion and cation (i.e. Zn^{2+}, Na^+, H^+) intercalation into the Mn-based cathodes, in which complex solid-phase behaviors cause limited capacity and poor reaction reversibility (**Figure 2**).

Recently, Cui and coworkers[76] proposed and demonstrated a completely different charge storage mechanism based on the liquid/solid Mn^{2+}/MnO_2 deposition/stripping chemistry, in which the discharged state is soluble Mn^{2+} aqueous solution and the charged state is solid-state MnO_2 (Figure 2). Using a new full cell chemistry of manganese dioxide-hydrogen gas (MnO_2-H_2) battery as an example, it achieved high cathode specific capacity and ultrastable cycling performance (10 000 cycles). This study evoked significant research interest in the exploration of the cathode Mn^{2+}/MnO_2 deposition/stripping chemistry to combine with a variety of anode chemistries, creating different Mn-based batteries such as MnO_2-Zn,[77–79] MnO_2-Cu,[80,81] MnO_2-Carbon,[82] and MnO_2-Pb,[83] to name a few, with superb electrochemical performance. Although the development of the Mn^{2+}/MnO_2 deposition/stripping chemistry is at its early stage, it presents great opportunities for the design of high-performance Mn-based batteries for practical large-scale energy storage applications.

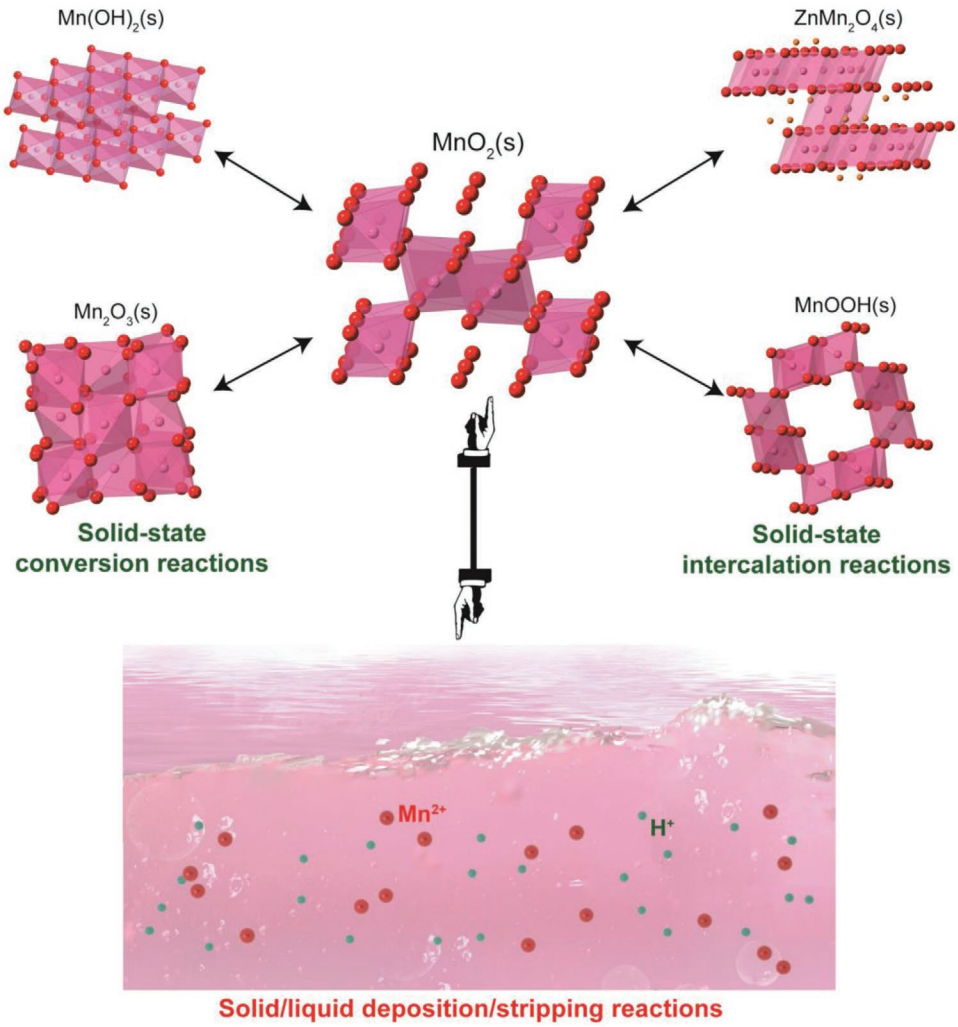

Figure 2. Charge storage mechanisms in aqueous Mn-based batteries. The development of Mn-based batteries can be classified by the storage mechanisms, which include, solid-state conversion and intercalation reactions and solid/liquid deposition/stripping reactions, the latter being the storage mechanism of the new generation Mn-based batteries.

This review aims to discuss the recent advances in the current state-of-the-art rechargeable aqueous Mn-based batteries with the new Mn^{2+}/MnO_2 chemistry. The development of the Mn-based batteries with different storage mechanisms is illustrated, with a focus on the latest generation Mn-based batteries in the Mn^{2+}/MnO_2 chemistry. In addition, we present the current understanding of the emerging Mn^{2+}/MnO_2 storage mechanism by a combination of advanced characterization techniques with simulation and theoretical calculation. The potential large-scale energy storage applications of the Mn-based batteries are also discussed. Furthermore, opportunities and future directions on the development of aqueous Mn-based batteries with the Mn^{2+}/MnO_2 chemistry are proposed.

2. The Development of Mn-Based Batteries with Different Mechanisms

As depicted in Figure 2, the Mn-based batteries have gone through two major generations that are characterized by their distinct charge storage mechanisms.[84–87] The first generation Mn-based batteries are based on the solid-state conversion and intercalation reactions of MnO_2 cathode, where alkaline and mild aqueous electrolytes are typically utilized.[88,89] The new generation Mn-based batteries are based on the cathode Mn^{2+}/MnO_2 deposition/stripping chemistry, where acidic aqueous solutions are generally required to realize the efficient deposition/stripping reactions.[76]

Since the discovery of the primary MnO_2-Zn battery,[61,90] the very first generation Mn-based batteries (Generation 1A) were typically operated in alkaline electrolytes.[91] However, they typically showed limited capacities and poor cycling performance.[92,93] The general failure mechanism of MnO_2 cathode in the alkaline electrolyte is ascribed to the partial irreversible conversion reactions between MnO_2 and the reduced Mn_2O_3 and $Mn(OH)_2$, or the gradual dissolution of MnO_2 into the strong alkaline electrolytes (Figure 2).[94–98] In order to improve the MnO_2 cathode instability issue, researchers have developed various strategies such as utilizing mixed KOH and LiOH instead of pure KOH as the electrolyte,[99–101] or different metals doping of MnO_2.[102–105] It was found that the battery capacity retention

rate and the number of cycles can be largely increased. In the case of mixed KOH and LiOH electrolyte, the enhancement of cycle performance is attributed to the formation of reversible Li_xMnO_2 ($0 < x < 1$) by lithium ion insertion into the MnO_2. Hertzberg and coworkers[92] used the alkaline electrolyte mixture of KOH and LiOH with a molar ratio of 1:3 to study the performance of MnO_2-Zn battery. Results showed that the battery can run over 60 cycles with capacity of ≈150 mAh g^{-1}, better than the cell in pure KOH electrolyte. In addition, some researchers have confirmed that the alkaline MnO_2-Zn battery is rechargeable for extended cycles by using a shallow cycle protocol which is typically less than 0.2–0.5 electron transfer per MnO_2.[106,107] However, the delivered capacity was very limited at the shallow depth of discharge such as 10%.[108] Attempt to achieve high capacity MnO_2 cathodes in alkaline electrolytes have been demonstrated to be effective by different metal doping into the MnO_2 structures. Wroblowa, Conway and coworkers[109,110] found that the alkaline MnO_2-Zn batteries with a small amount of bismuth doped MnO_2 cathode showed a relatively stable lifetime of up to 1000 cycles with about 80% of two-electron capacity of 616 mAh g^{-1}. However, these alkaline Bi/MnO_2-Zn batteries need to be operated by deploying ion-selective membranes to block the ZnO_2^{2-} ion transfer from the Zn anode to the MnO_2 cathode, and their operational voltages are ≈300 mV lower than the typical alkaline MnO_2-Zn batteries. In 2016, Banerjee and coworkers[105] synthesized a Cu ion intercalated Bi/MnO_2 that showed nearly two-electron charge capacity, high areal capacity of more than 20 mAh cm^{-2}, excellent rate performance and a stable lifetime of more than 6000 cycles, which demonstrated promising advancement toward the widespread applications of the alkaline MnO_2-Zn batteries.

The solid-state cation intercalation storage mechanisms in mild aqueous electrolytes account for the advanced first-generation Mn-based batteries (Generation 1B), which is dominated by the MnO_2-Zn battery chemistry.[111–116] In the 1980s, Yamamoto and coworkers[117,118] introduced the concept of a rechargeable MnO_2-Zn battery in a mild aqueous electrolyte of $ZnSO_4$, which showed operational voltage of 1.4 V and relatively good reversibility of 30 cycles. Later, Kang and coworkers[89] expanded this MnO_2-Zn battery chemistry with intercalation mechanism by using mild $ZnSO_4$ or $Zn(NO_3)_2$ solutions as the electrolyte. At the cathode Zn^{2+} can be reversibly intercalated into the tunnels of α-MnO_2, and the anode zinc can be electrochemically stripped to Zn^{2+} and deposited back reversibly.[119,120] The battery showed a relatively large capacity of 210 mAh g^{-1} and decent capacity retention at low charge/discharge rates.[89] However, the MnO_2-Zn batteries with the solid-state intercalation mechanism in mild aqueous electrolytes exhibited low capacities at high charge/discharge rates and significant capacity decay for long-term cycling. To elucidate the failure mechanism, a variety of ex situ and in situ techniques were conducted but controversial mechanisms were proposed by different groups.[79,121–125] For example, Kang and coworkers[89] proposed the Zn^{2+} insertion/extraction mechanism in the MnO_2-Zn batteries in mild $ZnSO_4$ or $Zn(NO_3)_2$ electrolyte by the demonstration of reversible Zn^{2+} insertion and desertion into/out of α-MnO_2 with the assistance of ex situ X-ray diffraction (XRD). However, Liu and coworkers[113] proposed the mechanism of reversible H^+ insertion/extraction reactions that were accompanied by the deposition of $Zn_4(SO_4)(OH)_6 \cdot nH_2O$ in the electrolyte of $ZnSO_4$ with a $MnSO_4$ additive *via* transmission electron microscopy. Though complicated due to different phases and structures of MnO_2 materials and complex battery systems, it is generally accepted that the proton insertion into the MnO_2 cathode promotes the reversibility of the Mn-based batteries in mild aqueous electrolytes (Figure 2).[113,126–128] Wang and coworkers[126] reported a MnO_2-Zn battery in a mild electrolyte, where the $MnSO_4$ was added into $ZnSO_4$ solution to inhibit the dissolution of MnO_2 during the cycling.[113,129,130] The electrochemical and structural analysis identified that the MnO_2 cathode underwent a consequent H^+ and Zn^{2+} insertion/extraction process with high reversibility and cycling stability.[131] In order to further improve the electrochemical performance of the Mn-based batteries in mild aqueous electrolytes, Chen and coworkers[132] reported a rechargeable aqueous MnO_2-Zn battery with 3 M $Zn(CF_3SO_3)_2$ and 0.1 M $Mn(CF_3SO_3)_2$ additive as the electrolyte, which delivered a highly reversible capacity of 225 mAh g^{-1} and 94% capacity retention after 2000 cycles. It is subjected to the bulky anion $CF_3SO_3^-$ that is beneficial to the reactivity and stability of the Zn anode and the spinel $ZnMn_2O_4$ cathode,[133] where the pre-added $Mn(CF_3SO_3)_2$ can effectively hamper the MnO_2 dissolution, and the electrode integrity can be maintained because of the in situ generated amorphous MnO_x layer in the charge process. Although the capacity and long-term cycling performance of the Mn-based batteries have been greatly improved with the intercalation storage mechanism in mild aqueous electrolytes, it is still desirable to develop novel Mn-based batteries chemistry with high output voltage and energy density to fulfill the extensive promotion of the large-scale energy storage market.[134–136]

The development of the new generation Mn-based batteries stems from the cathode Mn^{2+}/MnO_2 deposition/stripping chemistry (Generation 2) proposed by Cui and coworkers in 2017 (**Figure 3**a).[76] Although the Mn^{2+}/MnO_2 chemistry has been studied previously,[137–140] it is more related to the mechanism of MnO_2 electrodeposition, and it has not yet been deployed in the battery field due to unsatisfactory electrochemical performance. Since then researchers from all over the world have applied this emerging Mn^{2+}/MnO_2 storage mechanism to a variety of Mn-based batteries including MnO_2-Zn,[77,79] MnO_2-Cu,[80,81] MnO_2-Bi,[141] MnO_2-Pb,[83] and MnO_2-carbon[82] and achieved unprecedented electrochemical performance, as shown in the chronological development of Mn-based batteries (Figure 3a). Figure 3b shows a summary of the redox reactions and electrochemical potentials of the cathode Mn^{2+}/MnO_2 and different anodes which it can be paired with. These cathode and anode combinations provide new opportunities for the development of Mn-based batteries with low cost, high discharge potential, large capacity, high energy density, and long cycle life. **Table 1** shows a summary of the two generations Mn-based batteries with their cell parameters and electrochemical performance in different electrolytes. With the gradual development of the storage mechanism, the Mn-based battery performance in terms of output voltage, capacity, and energy density has been greatly improved, reaching the highest values in the new generation thanks to the cathode Mn^{2+}/MnO_2 chemistry. The emerging Mn^{2+}/MnO_2 energy storage mechanism is gaining reviving attention as promising redox chemistry for the development of the state-of-the-art aqueous Mn-based batteries.

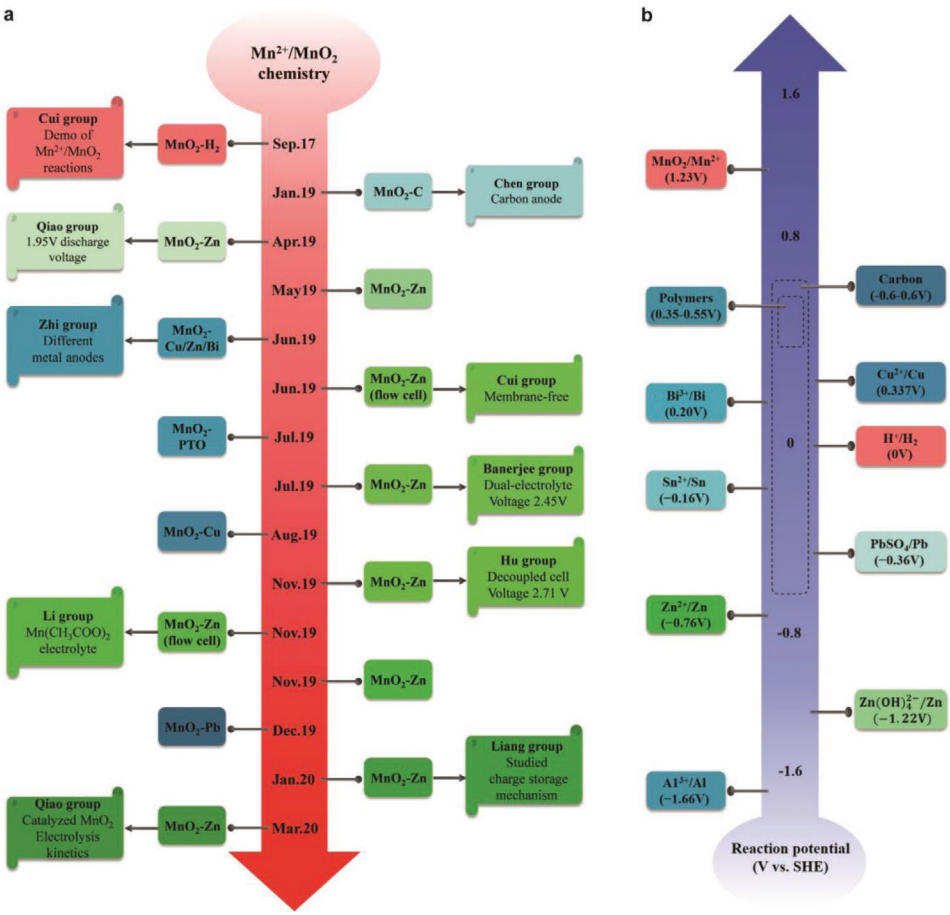

Figure 3. Development of new generation Mn-based batteries with Mn^{2+}/MnO_2 chemistry. a) Historical timeline for the development of the new generation Mn-based batteries with Mn^{2+}/MnO_2 storage mechanism. b) Redox reactions of the Mn^{2+}/MnO_2 cathode and different anodes with their theoretical electrochemical potentials as reported in literature.

3. Aqueous Mn-Based Batteries with Mn^{2+}/MnO_2 Chemistry

3.1. MnO_2-Hydrogen Gas Battery

The cathode Mn^{2+}/MnO_2 deposition/stripping reactions were initially demonstrated in the MnO_2-H_2 battery by coupling it with a catalytic hydrogen gas anode as reported by Cui and coworkers.[76,142,143] The cathode reactions were conducted between soluble Mn^{2+} and solid MnO_2 by reversible deposition/stripping, which is fundamentally different from the traditional solid-state cathode reactions in the first generation Mn-based batteries. The electrochemical reactions of the MnO_2-H_2 battery can be described in the following:

$$\text{Cathode}: Mn^{2+} + 2H_2O \leftrightarrow MnO_2 + 4H^+ + 2e^- \quad E_0 = 1.228\ \text{V vs SHE} \tag{1}$$

$$\text{Anode}: 2H^+ + 2e^- \leftrightarrow H_2 \quad E_0 = 0\ \text{V vs SHE} \tag{2}$$

$$\text{Overall}: Mn^{2+} + 2H_2O \leftrightarrow MnO_2 + 2H^+ + H_2 \quad E = 1.228\ \text{V} \tag{3}$$

The MnO_2-H_2 battery consists of a cathode-less porous carbon felt, a Pt/C catalyst-coated carbon felt anode, a glass fiber separator placed between the cathode and anode, and the aqueous $MnSO_4$ electrolyte. During charge, the soluble Mn^{2+} in the electrolyte was oxidized and coated on the cathode in the form of MnO_2, and hydrogen gas was generated from the anode under the active electrocatalysts. During discharge, the deposited MnO_2 was stripped back into the electrolyte, and hydrogen gas was oxidized on the anode. When using the electrolyte of 1 M $MnSO_4$ with 0.05 M H_2SO_4, the MnO_2-H_2 battery exhibited a discharge potential of ≈1.3 V (**Figure 4**b), fast rates up to 100 C, and a lifetime of over 10 000 cycles without decay at a current density of 10 mA cm^{-2} (Figure 4c). However, when cycled in pure $MnSO_4$ electrolyte without H_2SO_4, the MnO_2-H_2 battery showed gradual capacity decay over cycling. This is due to the synergetic effects of the cathode and anode reactions in the H_2SO_4 additive electrolyte, where higher electrolyte conductivity contributes to faster Mn^{2+}/MnO_2 reactions on the cathode and more favorable hydrogen evolution and oxidation reactions on the anode. In addition, it was confirmed that protons help promote the dissolution of MnO_2 in the discharge process and reduce the cell overpotential.[78] This

Table 1. Summary of the parameters and electrochemical performance of Mn-based batteries with different storage mechanisms.

Electrolyte	pH	Cathode	Anode	Discharge voltage (V)	Capacity [mAh g^{-1}]	Retention/Cycles (rate)	Ref.
Generation 1A: Alkaline electrolytes							
4 м KOH	≈13.5	MnO_2/Bi_2O_3	Zn plate	–0.3 vs Hg/HgO	230 (C/3)	0/15 (C/3)	[92]
1 м KOH + 3 м LiOH	≈13.2	MnO_2/Bi_2O_3	Zn plate	–0.3 vs Hg/HgO	300 (C/3)	43%/60 (C/3)	[92]
Saturated LiOH + 1 м $ZnSO_4$	≈8.5	MnO_2	Zn plate	1.60	148	20%/50	[99]
1 м NaOH or 9 м KOH	≈14	MnO_2	CMC-gell Zn powders	–0.4 vs Hg/HgO	N/A	N/A	[174]
7 м KOH	≈14	MnO_2	Zn foil	1.40	330	80%/2	[102]
Saturated LiOH + 1 м $ZnSO_4$	≈8.5	MnO_2-BGM	Zn plate	1.60	165	65%/2	[100]
1 м KOH + 3 м LiOH	≈14.6	β-MnO_2/Bi_2O_3	Zn plate	1.12	316	100%/100 (C/10)	[175]
40 wt% KOH	≈14	γ-MnO_2 nanowires	Zn powders	1.2	280	31 h (100 mA)	[176]
9 м KOH	≈14.6	$Ag_4Bi_2O_5$-MnO_2	N/A	1.2	481	≈34%/115 (1000 mA g^{-1})	[177]
15–45 wt% KOH	12–14	Cu-Bi-birnessite	Zn/ZnO	1.1	616	81%/900	[178]
9 м KOH	≈14.6	CM-MnO_2	Zn	1.00	492(1C)	40%/1000	[109]
45 wt% KOH	≈14.5	MnO_2	Zn/ZnO nickel mesh	1.43	31	80%/3000 (C/2)	[108]
25 wt% KOH	≈14.3	Cu-Bi-birnessite	NiOOH	–0.4 vs Hg/HgO	616	6000 (40C)	[105]
25 wt%KOH	≈14.3	MnO/Bi_2O_3	CNT-Zn	–0.5 vs Hg/HgO	750	80%/350(C/4)	[179]
Generation 1B: Mild aqueous electrolytes							
1 м $ZnSO_4$	≈4.0	α-MnO_2	Zn-birnessite	1.25	195 (C/20)	70%/30	[49]
0.1 м $Zn(NO_3)_2$	≈5.2	α-MnO_2	Zn foil	1.4	210 (0.5 C)	100%/100 (6 C)	[89]
1 м $ZnSO_4$	≈4.0	α-MnO_2	Zn foil	1.3	115 (83 mA g^{-1})	36%/75 (83 mA g^{-1})	[114]
1 м $ZnSO_4$	≈4.0	δ- MnO_2	Zn foil	1.38	112 (83 mA g^{-1})	44%/100 (83 mA g^{-1})	[115]
1 м $ZnSO_4$	≈4.0	α-MnO_2	Zn foil	1.3	233 (83 mA g^{-1})	63%/50 (83 mA g^{-1})	[111]
1 м $ZnSO_4$	≈4.0	α-MnO_2	Zn foil	1.4	108 (C/2)	43/50 (C/2)	[112]
2 м $ZnSO_4$ + 0.1 м $MnSO_4$	≈3.8	α-MnO_2	Zn foil	1.44	160 (5C)	92%/5000 (5 C)	[113]
2 м $ZnSO_4$	≈3.6	γ-MnO_2	Zn plate	1.3	119 (2 mA)	83%/30 (2 mA)	[118]
1 м $ZnSO_4$ + 0.1 м MnSO4	≈3.9	MnO_2-birnessite	Zn foil	1.39	505.9 (200 mA g^{-1})	100%/400 (500 mA g^{-1})	[131]
2 м $ZnSO_4$ + 0.1 м $MnSO_4$	≈3.8	MnO_2	Zn foil	1.35	220 (60 mA g^{-1})	95%/100 (60 mA g^{-1})	[129]
2 м $ZnSO_4$ + 0.2 м $MnSO_4$	≈3.6	MnO_2/graphene	Zn foil	1.4	382.2 (3A g^{-1})	94%/3000 (3A g^{-1})	[130]
3 м $Zn(CF_3SO_3)_2$ + 0.1 м $Mn(CF_3SO_3)_2$	≈3.3	β-MnO_2	Zn foil	1.4	225 (6.5 C)	94%/2000 (6.5 C)	[132]
3 м $Zn(CF_3SO_3)_2$	≈3.6	$ZnMn_2O_4$/C	Zn foil	1.4	150 (50 mA g^{-1})	94%/500 (500 mA g^{-1})	[133]
2 м $ZnSO_4$ + 0.1 м $MnSO_4$	≈3.8	PANI-MnO_2	Zn foil	1.36	290	96%/200 (200 mA g^{-1})	[180]
Generation 2: Acidic electrolytes with Mn^{2+}/MnO_2 reactions							
1 м $MnSO_4$ + 0.05 м H_2SO_4	≈1.0	Carbon felt	Pt/C-carbon felt	1.3	226.2 (10 mA cm^{-2})	100%/10 000 (10 mA cm^{-2})	[76]
1 м $ZnSO_4$ + 1 м $MnSO_4$ + 0.1 м H_2SO_4	≈1.1	Carbon fiber cloth	Zn foam	1.95	570 (2 mA cm^{-2})	92%/1800 (30 mA cm^{-2})	[79]
1 м $MnSO_4$ + 1 м $ZnSO_4$	≈3.8	Carbon felt	Zn foil	1.78	0.5 mA cm^{-2} (6 C)	100%/1000 (4 C)	[78]
0.5 м $MnSO_4$ + 2.8 м H_2SO_4	≈0.1	Carbon felt	Carbon felt	1.63	3.7 Ah L^{-1} (20 mA cm^{-2})	91.5%/100 (10 mAh cm^{-2})	[81]
1 м Na_2SO_4 + 1 м $MnSO_4$ + 0.1 м H_2SO_4	≈1.1	Graphite felt	Activated carbon	1.2	42.3	100%/7000 (1 mAh cm^{-2})	[82]
2 м $ZnSO_4$ + 1 м $MnSO_4$	≈3.3	MnO_2	CNT/Zn	1.5	0.96 mAh cm^{-2} (1 mA cm^{-2})	100%/11 000 (5 mA cm^{-2})	[134]
2 м $MnSO_4$ + 2 м H_2SO_4	≈0.15	MnO_2@graphite felt	PTO	0.82	150 (0.4 mA cm^{-2})	80%/5000 (2.5 C)	[153]
1 м $MnSO_4$ + 0.5 м H_2SO_4	≈0.5	Carbon cloth	Zn foil	2.42	621 (2 mA cm^{-2})	97.5%/6000 (2 mA cm^{-2})	[77]
0.8 м $MnSO_4$ + 0.1 м H_2SO_4	≈0.7	MnO_2@Carbon felt	Zn foil	2.45	308	100%/35 (C/2)	[150]
0.1 м $MnSO_4$ + 3 м H_2SO_4	≈0.1	MnO_2@Carbon felt	Zn foil	2.71	616 (100 mAh g^{-1})	98%/200 h (500 mAh g^{-1})	[151]
3 м $MnSO_4$ + 0.3 м H_2SO_4 + 0.06 м $NiSO_4$	≈0.5	Ni-MnO_2@Carbon felt	Zn foil	2.44	270 (2 C)	99%/450 (2 C)	[147]

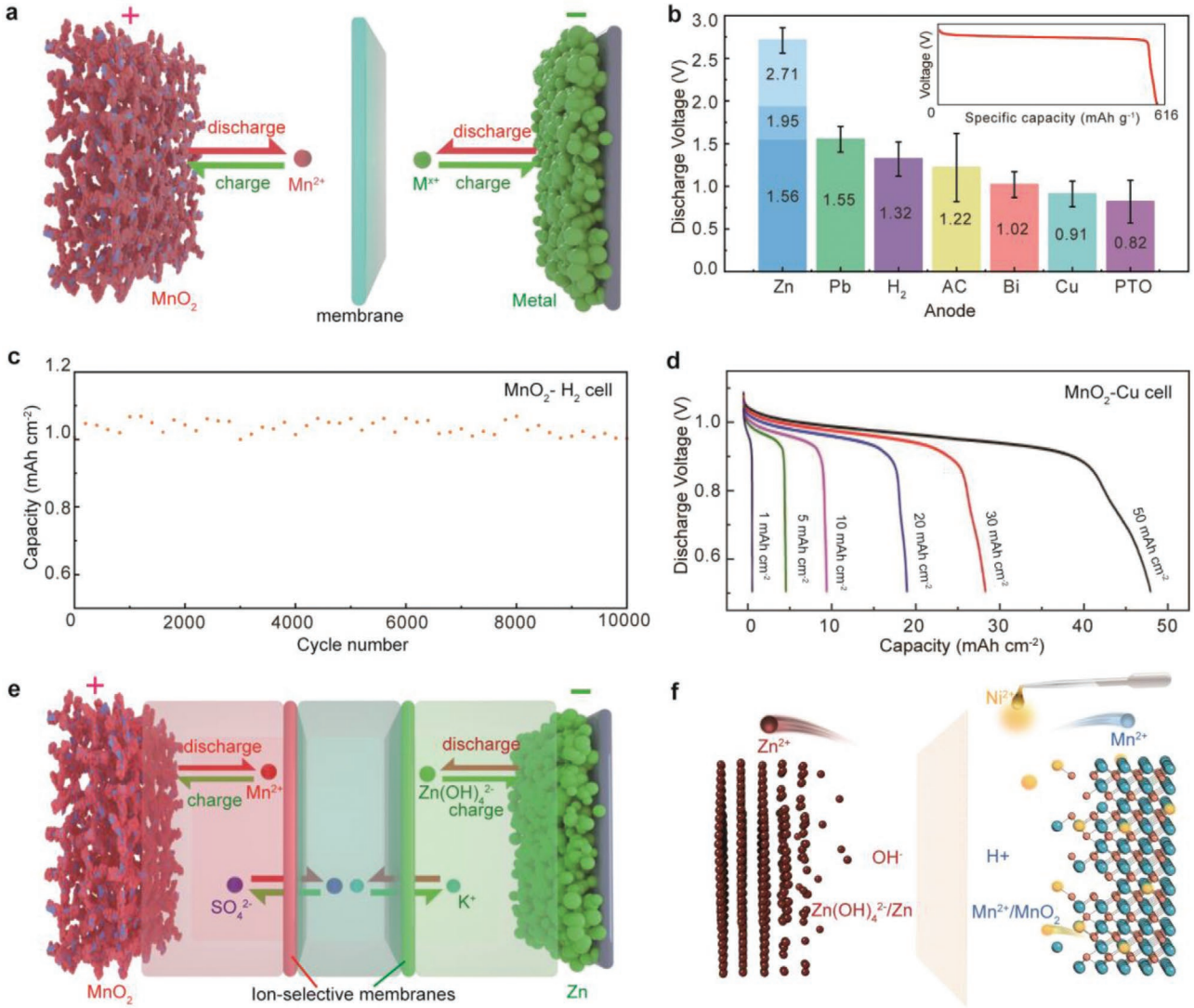

Figure 4. The aqueous Mn-based batteries with Mn^{2+}/MnO_2 chemistry. a) Schematic of the MnO_2-M (M: H_2, Zn, Cu, Pb, Sn, Bi, carbon, polymers, etc.) batteries with the Mn^{2+}/MnO_2 chemistry and their working mechanisms. b) The statistics of the discharge voltages of different MnO_2-M batteries that were reported in literature. The inset shows a typical discharge curve of the MnO_2-M batteries with a pronounced discharge plateau and the discharge capacity of ≈616 mAh g^{-1} is calculated based on the deposited MnO_2 with two-electron transfer of the Mn^{2+}/MnO_2 reactions. c) The long-term cycle stability of the MnO_2-H_2 battery, showing 10 000 cycles with negligible capacity decay. Reproduced with permission.[76] Copyright 2018, Springer Nature Ltd. The MnO_2-H_2 battery was tested at a constant charge potential of 1.6 V to 1 mAh cm^{-2} and discharged at 10 mA cm^{-2} to 0.5 V. d) The discharge curves of the MnO_2-Cu battery under different charge capacities, ranging from 1 up to 50 mAh cm^{-2}. Reproduced with permission.[80] Copyright 2019, Elsevier. e) Schematic of the electrolyte decoupled MnO_2-Zn battery with the cathode Mn^{2+}/MnO_2 chemistry and its working mechanism. f) Schematic of the electrolyte decoupled MnO_2-Zn battery with catalyzed electrolysis kinetics via facile introduction of Ni^{2+} into electrolyte. Reproduced with permission.[147] Copyright 2020, John Wiley and Sons.

work demonstrated exciting features of the cathode Mn^{2+}/MnO_2 deposition/stripping charge storage mechanism and the importance of electrolyte management for the development of the Mn-based batteries.

3.2. MnO_2-Zn Batteries

The excellent electrochemical performance of the MnO_2-H_2 battery with the cathode Mn^{2+}/MnO_2 chemistry has attracted much attention in the community of the Mn-based batteries. Therefore, researchers have applied the emerging cathode chemistry to many different Mn-based batteries. Owing to the abundance, high theoretical gravimetric capacity of 820 mAh g^{-1} and volumetric capacity of 5855 mAh cm^{-3} of the Zn metal anode, MnO_2-Zn batteries have been regarded one of the potential competitors for the grid-scale energy storage.[144–146] We discuss in this section the recent progress in MnO_2-Zn batteries using the cathode Mn^{2+}/MnO_2 chemistry.

Recently, Qiao and coworkers[79,147] reported an aqueous electrolytic MnO_2-Zn battery that was comprised of a Zn-foam anode, a glass fiber separator, a carbon fiber cloth as the cathode

substance and a mixture of $ZnSO_4$ with $MnSO_4$ aqueous electrolyte (Figure 4a). When charged at 2.2 V to a capacity of 2 mAh cm^{-2}, the MnO_2-Zn battery is capable of delivering an initial discharge capacity of 1.3 mAh cm^{-2}, which gradually increased to 1.92 and 1.97 mAh cm^{-2} in the 10th and 100th cycle, respectively. This result agrees well with the electrochemical behavior of the MnO_2-H_2 battery.[76] Three distinct regions with different electrochemical windows in the discharge curves were used to explain the energy storage mechanism of the MnO_2-Zn battery in the $ZnSO_4$ and $MnSO_4$ electrolyte. The first region (2–1.7 V) is responsible for the MnO_2/Mn^{2+} reaction, the second region (1.7–1.4 V) is dominated by the proton insertion into MnO_2, and the third region (1.4–0.8 V) is a result of the Zn^{2+} insertion into MnO_2. The storage mechanism was also confirmed by Liang and coworkers in their MnO_2-Zn battery.[148] In order to maximize the first high voltage region and minimize the inferior second and third regions, 0.1 M H_2SO_4 was added to the electrolyte of $ZnSO_4$ and $MnSO_4$ in the electrolytic MnO_2-Zn battery to facilitate the Mn^{2+}/MnO_2 deposition/stripping reactions. Therefore, the redox reactions of the MnO_2-Zn battery can be expressed in the following:

$$\text{Cathode}: Mn^{2+} + 2H_2O \leftrightarrow MnO_2 + 4H^+ + 2e^- \quad E_0 = 1.228\ \text{V vs SHE} \tag{4}$$

$$\text{Anode}: Zn^{2+} + 2e^- \leftrightarrow Zn \quad E_0 = -0.763\ \text{V vs SHE} \tag{5}$$

$$\text{Overall}: Mn^{2+} + Zn^{2+} + 2H_2O \leftrightarrow MnO_2 + Zn + 4H^+ \quad E = 1.991\ \text{V} \tag{6}$$

It exhibited much improved electrochemical performance such as a high discharge voltage of 1.95 V (Figure 4b), a high current density of 60 mA cm^{-2} and good cycling stability for over 1800 cycles. More importantly, the cost of this battery was estimated to be less than US$10 per kWh, far below that of the lithium ion and lead-acid batteries, showing its great potential for large-scale energy storage applications.[149] The electrolytic MnO_2-Zn technology is being industrialized by startups founded by the designers.

3.3. Electrolyte Decoupled MnO_2-Zn Battery

With the improved electrolyte optimization and management, the advantages of the cathode Mn^{2+}/MnO_2 chemistry have been further amplified. The reduction potential of Zn anode in alkaline electrolyte is –1.199 V (vs SHE), lower than that of the Zn anode in acidic electrolyte (–0.763 V vs SHE). In order to achieve high overall potential for the MnO_2-Zn battery, it is in principal feasible to build a battery by separating the cathode and anode in the acidic and alkaline electrolytes, respectively. In 2019, Banerjee and coworkers[150] reported for the first time the development of electrolyte-decoupled aqueous MnO_2-Zn batteries with high voltages of 2.45 and 2.8 V without the use of costly ion-selective membranes. The cathode was driven by the Mn^{2+}/MnO_2 deposition/stripping or Mn^{2+}/MnO_4^- chemistries in aqueous acidic electrolytes and the anode was driven by the $Zn/Zn(OH)_4^{2-}$ reactions in alkaline electrolyte. The cell was achieved by gelling the anode alkaline electrolyte and using low-cost cellophane separator to separate from the cathode aqueous acidic electrolyte. It is believed an important advance toward the fabrication of electrolyte-decoupled high-voltage aqueous MnO_2-Zn batteries. Liu and coworkers[77] built such a high-voltage aqueous MnO_2-Zn battery by using a bipolar membrane to separate the cathode and anode electrolytes in different pH environments. The MnO_2-Zn battery with the dual electrolytes showed a high discharge voltage of 2.42 V, high coulombic efficiency of 98.4% and stable cycling for 1500 cycles. Very recently, Hu and coworkers[151] developed a similar MnO_2-Zn battery with a two-membrane three-chamber design as shown in Figure 4e. The cathode MnO_2 in strong acidic chamber with an electrolyte of $MnSO_4$ and H_2SO_4 and the anode Zn in strong alkaline chamber with an electrolyte of KOH, ZnO, and vanillin were separated by a neutral chamber with an electrolyte of K_2SO_4, where cation and anion exchange membranes were placed in between. The central chamber in neutral electrolyte provides adequate intermediate space for the ions transportation to avoid the neutralization effect caused by the excessive pH difference of the acidic and alkaline electrolytes. The MnO_2-Zn battery with the decoupled stronger acidic and alkaline electrolytes showed a higher discharge voltage of 2.71 V than the previous design (Figure 4b). In addition, it showed 200 hours of high-current deep charge–discharge behavior, and stable cycling life of 1000 times with a 10% state of charge. Enabled by connecting cells in parallel and series, the stacked batteries showed capability to deliver high voltages and capacities. However, the usage of strong acid and alkaline electrolytes and the complex two-membrane three-chamber design will increase the difficulty on battery assembling, housing, and welding. Optimization of the battery system complexity in terms of electrolytes and cell structures are highly desirable to the mass production of the electrolyte-decoupled MnO_2-Zn batteries. Furthermore, the usage of two ion-selective membranes will worsen the kinetics and corresponding power density of the device. Further development of high-performance and cost-effective membranes will help improve the overall battery performance and lower the capital cost for practical applications of the electrolyte-decoupled MnO_2-Zn batteries. Recently, Qiao and coworkers reported an electrolyte decoupled MnO_2-Zn battery with catalyzed Mn^{2+}/MnO_2 electrolysis kinetics (discharge in 60 s, at 50 C) via facile introduction of trace amount of Ni^{2+} into the electrolyte (Figure 4f).[147] The hybrid aqueous battery demonstrated an electrochemical stability window of over 3.4 V and flat discharge voltage of 2.44 V.

3.4. Other Mn-Based Batteries with Mn^{2+}/MnO_2 Chemistry

The development of the MnO_2-Zn batteries with the cathode Mn^{2+}/MnO_2 chemistry has accelerated the fabrication of other Mn-based batteries. Copper (Cu) is an Earth-abundant inexpensive metal with high deposition/dissolution efficiency and dendrite-free morphology, large specific capacity of 843 mAh g^{-1}, and volumetric capacity of 7558 mAh cm^{-3}, making it a good battery anode material to be explored. Recently, by virtue of the reversible cathode Mn^{2+}/MnO_2 reactions, Zhi and coworkers[141] reported a rechargeable aqueous MnO_2-Cu battery. This MnO_2-Cu battery demonstrated energy

density of 27.7 mWh cm^{-2} and power density 1.232 W cm^{-2} with high reversibility. It can be charged to 0.8 mAh cm^{-2} within 42 s and has a good voltage platform of ≈0.95 V at 20 C. The results are consistent with the MnO_2-Cu batteries reported by Xia and coworkers[80] and Zhao and coworkers,[81] where a long life of 10 000 cycles without obvious capacity decay and a high discharge capacity of up to 50 mAh cm^{-2} were achieved respectively (Figure 4d). The excellent electrochemical performance of the MnO_2-Cu battery suggests its huge potential for large-scale energy storage applications. Other promising metals such as aluminum (Al), bismuth (Bi), and lead (Pb) were also employed as anode materials by pairing them with the cathode of Mn^{2+}/MnO_2 chemistry, naming MnO_2-Al,[152] MnO_2-Bi,[141] and MnO_2-Pb[83] batteries, showing favorable characteristics to be optimized for high-performance batteries.

In addition to the MnO_2-metal batteries, other anode materials can be utilized to design novel Mn-based batteries based on the Mn^{2+}/MnO_2 chemistry. Activated carbon (AC) as an excellent material that was widely used in supercapacitors, has been applied to the Mn-based batteries. Such a MnO_2-carbon battery was fabricated by using graphite felt as the cathode substance, AC as the anode and 1 M Na_2SO_4, 1 M $MnSO_4$ with 0.1 M H_2SO_4 as the electrolyte.[82] This battery was operated by the cathode Mn^{2+}/MnO_2 reactions and the anode Na^+ adsorption/desorption on the AC with high surface area. Due to the excellent reversibility of both the cathode Mn^{2+}/MnO_2 reactions and the anode ion adsorption/desorption, the MnO_2-carbon battery exhibited an average discharge voltage of 1.2 V (Figure 4b) and a cycle life of more than 7000 times. The hybridization of the battery-like Mn^{2+}/MnO_2 cathode with the supercapacitor-like carbon anode gives rise to a new category of Mn-based batteries with superior electrochemical performance.

Moreover, organic materials with good electrochemical properties have been applied to the Mn-based batteries with the cathode Mn^{2+}/MnO_2 chemistry. Wang and coworkers[153] reported an inorganic-organic MnO_2-PTO (pyrene-4,5,9,10-tetraone) battery, which was achieved by the cathode Mn^{2+}/MnO_2 reactions and the anode quinone/hydroquinone redox reactions through hydronium-ion transformation between the two electrodes. The hydronium-ion MnO_2-PTO battery exhibited a discharge platform of approximately 0.8 V (Figure 4b), and a cycle life of 5000 cycles with 99% of coulombic efficiency. Impressively, the battery survived at low temperature of –70 °C with preserved good capacity and cycling performance. Such a MnO_2-PTO battery with low-temperature tolerance may find crucial applications in extreme conditions and outer space.

3.5. MnO_2-Zn Flow Batteries

The exploration of Mn-based batteries with the cathode Mn^{2+}/MnO_2 chemistry has stimulated the development of Mn-based redox flow batteries. Redox flow battery is a rechargeable battery technology in which active substances exist in liquid electrolytes and are stored externally, enabling the separation of energy and power.[2] In addition, redox flow batteries have the characteristics of high safety, high efficiency, and long life, showing promises for large-scale energy storage.[154–157] The feasibility of redox flow MnO_2-Zn battery (**Figure 5**a) was first demonstrated by Qiao and coworkers.[79] A redox-flow battery stack with a capacity of 2 Ah was built, which demonstrated a practical strategy toward large-scale energy storage using the new electrolytic MnO_2-Zn system. The output voltage, energy efficiency, and cost of the flow-battery design were comprehensively analyzed, which perform better than conventional aqueous flow battery systems, such as Zn-Fe, Zn-Br_2, Zn-Ce, Zn-air, and all-vanadium flow batteries.[79] In a recent work, Li and coworkers[51] demonstrated a MnO_2-Zn flow battery by taking the advantages of the cathode Mn^{2+}/MnO_2 deposition/stripping reactions and the anode Zn^{2+}/Zn reactions. $Mn(CH_3COO)_2$ was selected as the active material for the catholyte. Due to the coordination effect of the CH_3COO^-, Mn^{2+} can be directly converted to MnO_2 and reversibly stripped back to Mn^{2+} even in the acid-free neutral electrolyte. The MnO_2-Zn flow battery exhibited a discharge platform of ≈1.56 V (Figure 4b), good rate performance and no significant capacity decay for over 400 cycles. However, the utilization of $Mn(CH_3COO)_2$ to replace $MnSO_4$ in the electrolyte has reduced the cell voltage by ≈530 mV. Therefore, further research is needed to improve the overall electrochemical performance and lower the cost of the conventional MnO_2-Zn flow battery. In these regards, Cui and coworkers[78] developed a membrane-free MnO_2-Zn flow battery by circulating the single electrolyte, instead of the separated catholyte and anolyte in the conventional flow battery, through one tank without using the relatively expensive ion selective membrane (Figure 5b). The membrane-free MnO_2-Zn flow battery was conducted by the cathode Mn^{2+}/MnO_2 reactions on carbon felt and the anode Zn^{2+}/Zn reactions on Zn foil in the electrolyte of 1 M $ZnSO_4$ and 1 M $MnSO_4$. By virtue of the electrolyte flow, the newly generated proton during the charge process can be evenly distributed, facilitating the dissolution of MnO_2 during the discharge process. The battery exhibited a high discharge voltage of ≈1.8 V (Figure 5c), good discharge rates from 0.5 to 10 C, and stable 1000 cycles with nearly 100% of coulombic efficiency (Figure 5d). The development of membrane-free MnO_2-Zn flow battery provides an economic strategy toward their large-scale energy storage applications.

4. Understanding of the Mn^{2+}/MnO_2 Storage Mechanism

Researchers have attempted to understand the Mn^{2+}/MnO_2 deposition/stripping mechanism from different aspects including ex situ and in situ characterizations, dynamic simulation, and theoretical calculation. In some early work, Donne and coworkers[137,140,158–162] studied the electrodeposition mechanism of MnO_2 in acidic and neutral media by using the techniques of rotating disk electrode and rotating ring-disk electrode,[140,158] indicating that the electrodeposition of MnO_2 is closely related to the pH value and dependent on the substrate. In addition, the electrochemical kinetic behavior of the MnO_2 cathode in aqueous solution was investigated to reveal the reduction process of MnO_2 via a series of constant current discharge experiments,[162] which helps the exploration of the Mn^{2+}/MnO_2 deposition/stripping mechanism. In terms of the battery characterization, a combination of different characterization tools is often involved in revealing the dynamic processes of the

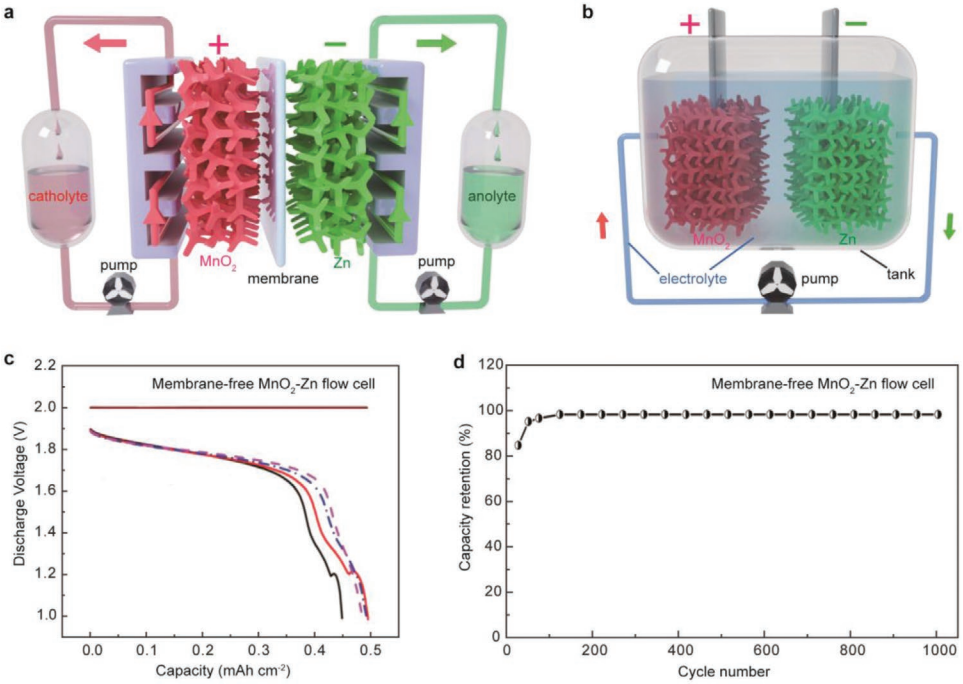

Figure 5. MnO_2-Zn flow batteries with cathode Mn^{2+}/MnO_2 chemistry. a) Schematic illustration of the conventional MnO_2-Zn flow battery. The cathode and anode are separated by a membrane. b) Schematic of the membrane-free MnO_2-Zn flow battery, which consists of a tank containing cathode, anode, and electrolyte, and the pump-drive electrolyte circulation system. c) The charge and discharge curves of the membrane-free MnO_2-Zn flow battery. The initial coulombic efficiency of the battery is ≈90%, but the capacity ramps up with the cycling and can reach theoretical value after the initial activation. d) The cycling stability behavior of the membrane-free MnO_2-Zn flow battery with capacity retention over 1000 cycles. The charge–discharge and cycling tests were performed at a constant charge potential of 2 V to 0.5 mAh cm^{-2} and a constant discharge rate of 4 C. Panel (c)and (d). Reproduced with permission.[78] Copyright 2020, John Wiley and Sons.

Mn^{2+}/MnO_2 reactions, which require high spatial and temporal resolutions. Scanning electron microscopy (SEM) provides a powerful opportunity for researchers to directly observe the evolution of the Mn^{2+}/MnO_2 reactions on the Mn-based battery cathode. Hu and coworkers[151] analyzed the morphology of the MnO_2 cathode by ex situ SEM at different depth of charge (DoC) and discharge (DoD) states in a complete charge/discharge cycle (**Figure 6**a). The cathode showed porous carbon nanoparticulate morphology before charge (Figure 6a, C1) and gradually coated with nanosheet-like MnO_2 deposits during charge until the pores and spaces between the carbon particles completely filled up, forming the heavily deposited MnO_2 cathode (Figure 6a, C2–C6). While during discharge, the interconnected MnO_2 particles on the cathode were gradually dissolved and reverted to the initial porous carbon nanoparticulate morphology (Figure 6b). The corresponding energy-dispersive X-ray spectroscopy, ex situ XRD, and X-ray photoelectron spectroscopy have quantitatively confirmed the highly reversible Mn^{2+}/MnO_2 reactions in each charge/discharge stages. Correspondingly, the electrolyte evolution over the entire charge/discharge processes has been monitored through a finite element simulation by modeling the dynamic $MnSO_4$ electrolyte concentration variation.[76] As shown in Figure 6c, the representative spectra of the Mn^{2+} concentration distribution demonstrated the fully recoverable spatial variation of the electrolyte concentration after the complete charge/discharge cycle, suggesting the highly reversible Mn^{2+}/MnO_2 reactions. This agrees well with the evolution of the Mn^{2+}/MnO_2 reactions on the Mn-based battery cathode. Experimentally, the concentrations of the Mn^{2+} in the electrolyte during charge/discharge processes were measured by plasma optical emission spectroscopy (ICP-OES),[151] which were consistent with the calculated theoretical concentrations from the amount of deposited MnO_2, conforming the highly reversible Mn^{2+}/MnO_2 reactions.

In addition, in situ Raman spectroscopy was applied to probe the deposited MnO_2 on the cathode carbon substrate of the MnO_2-Zn battery in operation (Figure 6d).[151] The characteristic peak of MnO_2 at 572 cm^{-1} appears immediately at the beginning of the charge process, which indicates that MnO_2 is being deposited, until it is suddenly disappeared at the end of the discharge process where the discharge potential dropped rapidly, which is accompanied by the appearance of the characteristic carbon peaks at 1354 and 1598 cm^{-1}, indicating the complete MnO_2 dissolution from the cathode and the exposure of the underlying carbon substrate. This further confirmed the highly reversible Mn^{2+}/MnO_2 reactions.

Density functional theory (DFT) calculations were performed to understand the energy storage mechanism of the Mn^{2+}/MnO_2 redox reactions in acidic electrolytes.[79] It was suggested by electron energy loss spectrum (Figure 6e) that the deposited MnO_2 in the acidic electrolyte of $MnSO_4$ with 0.1 M H_2SO_4 contains Mn vacancies as opposed to the deposited MnO_2 without H_2SO_4. The Mn vacancies were directly observed by a high-angle annular dark-field scanning

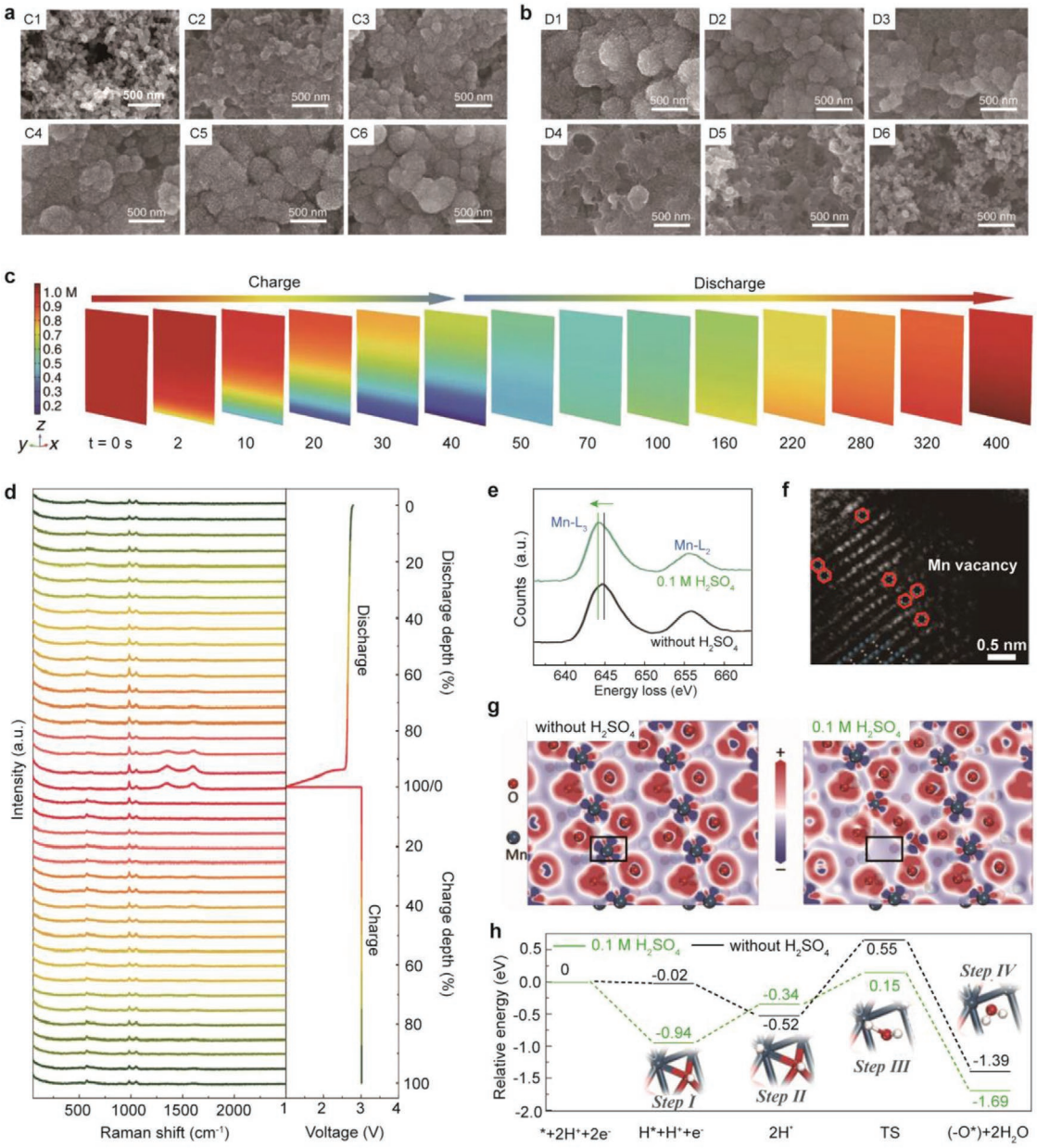

Figure 6. Energy storage mechanism of the Mn^{2+}/MnO_2 chemistry revealed by characterization, simulation, and theoretical calculation. a) SEM images of the MnO_2 electrode after charge at DoCs of 0 (C1), ≈20% (C2), ≈40% (C3), ≈60% (C4), ≈80% (C5), and ≈100% (C6) at a charge voltage of 3 V. b) SEM images of the MnO_2 electrode after discharge at DoDs of 0 (D1), ≈20% (D2), ≈40% (D3), ≈60% (D4), ≈80% (D5), and ≈100% (D6) at a current density of 200 mA g^{-1}. c) Finite-element analysis of the cathode Mn^{2+}/MnO_2 deposition/stripping reactions by the simulation of dynamic electrolyte concentration variation over an entire charge–discharge process. The model was built in COMSOL software based on a cell with a cathode and an anode in square shape of 250 µm × 250 µm, and the electrolyte with thickness of 350 µm which is equivalent to the separator was used to set them apart. The resulting representative spectra correspond to different charge–discharge durations were obtained under a constant charge potential of 1.6 V to a capacity of 1 mAh cm^{-2} and a discharge current density of 10 mA cm^{-2} in 1 M $MnSO_4$ electrolyte. Detailed information about the modelling is available in ref. [76]. d) In situ Raman spectra of the MnO_2 cathode in the charge/discharge processes. The measurements were performed on the decoupled MnO_2-Zn battery at a charge potential of 3 V and a discharge current density of 200 mA g^{-1}. e) Mn-$L_{2,3}$ EELS spectra of the deposited MnO_2 with and without 0.1 M H_2SO_4 addition in the electrolytes. The shift of Mn-L_3 main peak of MnO_2 from 644.9 eV (without 0.1 M H_2SO_4) to 644.3 eV (with 0.1 M H_2SO_4) and the higher L_3/L_2 integral peak intensity ratio of MnO_2 in 0.1 M H_2SO_4 imply the reduction of Mn valence state and the existence of Mn^{3+} in MnO_2 that was deposited in the electrolyte with 0.1 M H_2SO_4 addition. f) Atomic-resolution HAADF-STEM image of the deposited MnO_2 with Mn vacancies (marked in red hexagons). g) Electron density variation of the MnO_2 with (in 0.1 M H_2SO_4) and without Mn vacancies (without H_2SO_4). The Mn vacancy is marked with a black rectangular in MnO_2 with 0.1 M H_2SO_4 on the right image. h) Relative energy profiles of the MnO_2 dissolution reaction pathway with four subsequent steps. Insets are the schematics of the MnO_2 crystal structure changes in the four reaction steps from I to IV. Mn, O, and H atoms are labeled as blue, red, and white balls, respectively. Detailed explanation of the four reaction steps is available in ref. [79]. Panel (a), (b), and (d). Reproduced with permission.[151] Copyright 2020, Springer Nature Ltd. Panel (c). Reproduced with permission.[76] Copyright 2018, Springer Nature Ltd. Panel (e), (f), (g), and (h). Reproduced with permission.[79] Copyright 2019, John Wiley and Sons.

transmission electron microscope image (Figure 6f), which was performed on a high-resolution aberration-corrected transmission electron microscope. It was further analyzed that the deposited MnO_2 with Mn vacancies has a higher diffusion coefficient and a lower overpotential than that of the pristine MnO_2. Such Mn vacancies were believed to facilitate the generation of unsaturated oxygen species and help offer additional pathways for cations with higher mobility in the aqueous electrolytes. The DFT calculation revealed that the surface electron density tends to increase on the Mn vacancies, which helps reduce the reaction energy barrier and accelerate the electron transfer dynamics (Figure 6g). In this respect, the reaction pathway of the MnO_2 dissolution with the assistance of Mn vacancies, which involves four major steps, proceeds in promoted reaction dynamics with lower overpotentials (Figure 6h). Recently, the Ni catalyzed Mn^{2+}/MnO_2 electrolysis kinetics process was carefully explored by Qiao and coworkers with the help of synchrotron spectra techniques and DFT calculations.[147] The significant role of Ni introduction in powering electrolytic reactivity is proposed via enhanced active electron states, charge delocalization, and facilitated charge-transfer around strong electronegativity Ni.

5. Toward Large-Scale Energy Storage Applications

Owing to the remarkable advantages of low cost, good safety, high operation voltage, long lasting and reliable shelf life, high capacity, and energy density, the Mn-based batteries with the cathode Mn^{2+}/MnO_2 chemistry are promising for next-generation large-scale energy storage.[76,78] **Figure 7**a shows a conceptual schematic of the representative future

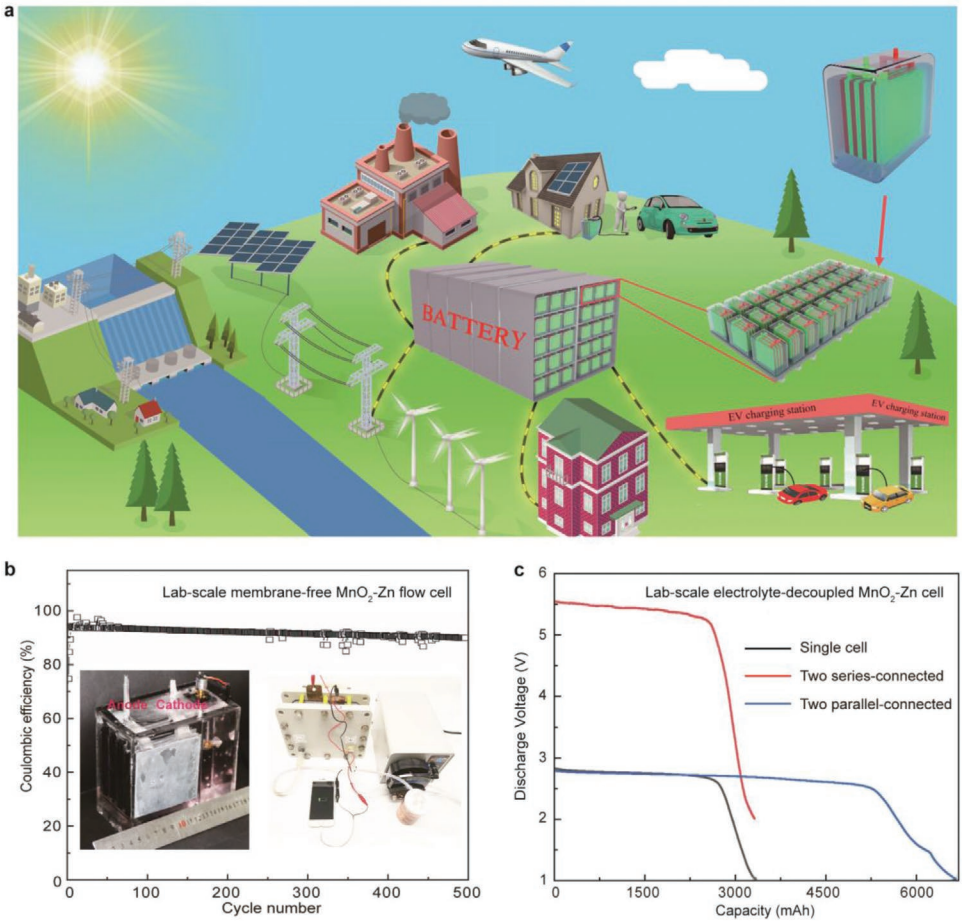

Figure 7. The grid-scale energy storage applications of Mn-based batteries with Mn^{2+}/MnO_2 chemistry. a) A conceptual schematic illustration of the future grid-scale energy storage applications of the rechargeable aqueous Mn-based batteries. It is achieved by the integration of renewable solar, wind and hydro powered electricity with the electrical grid, as well as, the transformation of the Mn-based battery technology with large scaling up and mass production from the research lab to industry. The grid-scale energy storage applications of the Mn-based batteries will benefit our society from individual households, transportations, factories, and buildings to the entire community. b) The long-term stability of a prototype membrane-free MnO_2-Zn flow battery over 500 cycles. The battery was charged at 2 V to 1200 mAh and then discharged at 1000 mA to 1 V for 500 consecutive times. Inset (left) is a digital photograph of the prototype lab-scaling-up membrane-free MnO_2-Zn flow battery with capacity of ≈1200 mAh. Reproduced with permission.[78] Copyright 2020, John Wiley and Sons. Inset (right) is a digital photograph of the prototype lab-scaling-up MnO_2-Zn flow battery with capacity of ≈2000 mAh. Reproduced with permission.[78] Copyright 2020, John Wiley and Sons. c) The discharge behaviors of the lab-scale decoupled MnO_2-Zn batteries with two different cell connections, for example, two series-connected and two parallel-connected cells. The single unit cell is a decoupled MnO_2-Zn battery with a theoretical capacity of 3370 mAh. Reproduced with permission.[151] Copyright 2020, Springer Nature Ltd.

grid-scale energy storage based on the rechargeable Mn-based batteries with the Mn^{2+}/MnO_2 chemistry. By virtue of integrating renewable yet intermittent energy resources such as solar, wind and hydro-electricity into electrical grid, the centralized Mn-based battery system with capacity of MWh can be used to power individual households, factories, buildings, and transportations like electric vehicles.[163] The Mn-based battery system plays a critical role as an indispensable supplement to the present electrical grid or even replaces it completely to achieve 100% green electricity in our society. In addition, the dispatchable Mn-based batteries can be functionalized as distributed utility energy resources and found applications wherever they are able to.

The realization of the proposed fascinating spectacle of the future sustainable energy storage applications becomes feasible when taking into account mass production of the Mn-based batteries. As depicted in Figure 7a, the Mn-based battery pack can be assembled on the basis of multiple stacks of batteries that are constructed by connecting a number of individual Mn cells in series and in parallel to deliver high current and voltage for practical applications. It can be achieved through mass production of the Mn-based batteries with progressive technology readiness levels from research lab to industry. In order to demonstrate the scalability of the Mn-based batteries with the Mn^{2+}/MnO_2 chemistry, a prototype lab-scale membrane-free MnO_2-Zn flow battery with a capacity of 1200 mAh has been fabricated by increasing the area of the cathode carbon substances, which demonstrated excellent electrochemical behaviors with stable cycle performance (Figure 7b).[78] Considering that it is a primary scale-up cell design that has not been optimized for maximum electrochemical performance, the Mn-based battery is believed to meet the requirements of large-scale energy storage after further improvement. In addition, the Mn-based batteries with the Mn^{2+}/MnO_2 chemistry are feasible to be greatly scaled up by various cell designs such as pouch and prismatic cell packs, providing high flexibility to the future Mn cell design and optimization of packaging efficiency at the battery level. For example, Xia and coworkers developed a MnO_2-Pb pouch cell[83] with a capacity up to 536 mAh and a Mn-Cu prismatic cell[80] with a capacity up to 6646 mAh, both of which showed good discharge properties with high coulombic efficiency. In another study, Hu and coworkers[151] fabricated a decoupled MnO_2-Zn battery with a high discharge voltage of ≈2.75 V by scaling up its capacity to 3330 mAh. As shown in Figure 7c, when connecting such two single cells in series, the output voltage of the battery was doubled and reaching ≈5.44 V without sacrificing the high capacity. While connecting two individual cells in parallel, the resulting battery showed capacity of ≈6660 mAh with similar discharge potential of ≈2.7 V. Furthermore, the battery pack which was formed by connecting several decoupled MnO_2-Zn cells in parallel and series, was integrated with a wind-driven generator and photovoltaic hybrid power generation systems to demontrate its practical energy storage capability. Previous successful integration of the renewable energy resources and the practical applications of the stored energy to power LED panel, cellphone, and vehicle model have demonstrated the significant potential of the Mn-based batteries with the Mn^{2+}/MnO_2 chemistry for large-scale energy storage.[76,78,79,147]

6. Opportunities and Future Perspectives

The continued pursuit of renewable battery technologies for large-scale energy storage will accelerate the exploration of the state-of-the-art rechargeable aqueous Mn-based batteries with the Mn^{2+}/MnO_2 chemistry. However, further research is required to effectively enable their practical applications for the benefit of society. Critical challenges include, but not limited to, understanding battery charge storage mechanism, achieving high electrochemical performance that complies with the best practice for measurements, incorporating theoretical calculation and simulation, exploring new Mn-based battery chemistry with the Mn^{2+}/MnO_2 chemistry, optimizing battery system integration, and applying the Mn-based batteries in large-scale applications via scaling up and commercialization (**Figure 8**). In this endeavor, it is highly desirable to develop future Mn-based batteries by considering the above-mentioned aspects in a holistic strategy.

6.1. Charge Storage Mechanism

Although the charge storage mechanism of the cathode Mn^{2+}/MnO_2 reactions has been primarily revealed by different characterization techniques, simulation and theoretical calculations, it is still necessary to understand the intermediate steps involving the complex Mn^{2+}/MnO_2 reactions toward two-electron charge-transfer in the charge and discharge processes from a battery level perspective. It was generally accepted that the Mn^{2+}/MnO_2 reactions are involved in multiple electrochemical and chemical redox reactions that are highly dependent

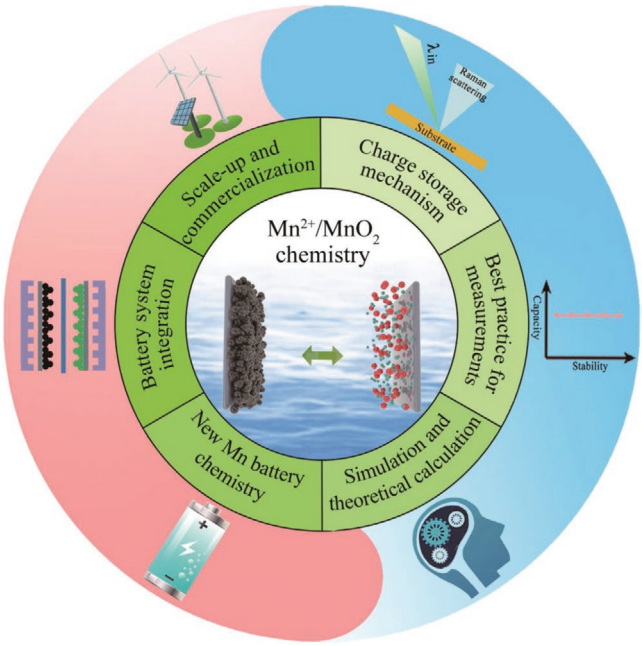

Figure 8. New opportunities for developing Mn-based batteries with the Mn^{2+}/MnO_2 chemistry, including charge storage mechanism, best practice for measurements, simulation and theoretical calculation, new Mn-based battery chemistry, battery system integration, and scale-up and commercialization for large-scale energy storage applications.

on the proton reactivity of the electrolytes and the charge/discharge parameters. These reactions include the electrochemical oxidation of Mn^{2+} to Mn^{3+}, the chemical hydrolysis of Mn^{3+} to MnOOH or the disproportionation of Mn^{3+} to form Mn^{2+} and Mn^{4+}, and the further electrochemical oxidation of MnOOH to MnO_2 or the hydrolysis of Mn^{4+} to MnO_2.[137–139] Due to the complex cathode Mn^{2+}/MnO_2 reactions paired with various anode reactions in the respective battery systems, there has been controversial regarding the Mn^{2+}/MnO_2 deposition/stripping mechanism on the reaction pathways and electron transfer. Therefore, some advanced in situ/operando characterization tools with high spatial and temporal resolutions should be applied to unveil the intrinsic storage mechanism of the cathode Mn^{2+}/MnO_2 reactions.[151,164,165] A number of in situ/operando techniques may provide powerful capabilities for understanding the energy storage mechanism of Mn-based batteries by addressing key issues of the Mn^{2+}/MnO_2 reactions regarding the identity and configuration of possible intermediates, preferred reaction pathways and impact of reaction conditions. The various techniques include in situ/operando infrared and Raman spectroscopies, electrochemical impedance spectroscopy, X-ray absorption spectroscopy, scanning probe microscopy, scanning electrochemical microscope, liquid-phase transmission electron microscopy, cryogenic-electron microscopy, and their rational combinations.[166,167] Besides the proton reactivity, the introduction of both other cations (Ni^{2+} and Zn^{2+}) and anions (sulfate and acetate) may result in different electrolysis kinetics.[51,147] These catalysis/passivation mechanisms with different solute and solvent are very interesting and should be carefully investigated to improve the electrochemical performance of Mn-based batteries further.

6.2. Best Practice for Measurements

A challenge to evaluate the electrochemical performance of Mn-based batteries with the cathode Mn^{2+}/MnO_2 reactions is the lack of standardized criteria regarding calculations and measurements. As a consequence, it is difficult and unreliable to compare the reported results from different studies, which will lead to unhealthy growth in this area. For the cathode Mn^{2+}/MnO_2 reactions which are typically conducted in $MnSO_4$ electrolyte, high theoretical specific capacity of ≈616 mAh g^{-1} is often reported based on the two-electron charge transfer reactions. Actually, defects cannot be eliminated in the derived Mn oxides via the electrodeposition process,[79,82] which makes the intrinsic valence state of Mn oxides lower than 4+ and results in a lower capacity than the theoretical value of 616 mAh g^{-1}. Moreover, when it comes to the concentration of the $MnSO_4$ electrolyte by considering the electrolyte mass and volume, the theoretical specific capacity of the Mn^{2+}/MnO_2 reactions drops to ≈141 mAh g^{-1} (volumetric capacity ≈214 Ah L^{-1}) with 100% DoD at a concentration of ≈4 M of $MnSO_4$ at room temperature.[76] As the cathode Mn^{2+}/MnO_2 reactions involve liquid/solid conversion, one is highly suggested to include the solute and solvent as a whole into consideration for the evaluation of battery performance such as gravimetric and volumetric capacity, energy and power densities. One general practice we urge is to clearly state the parameters of batteries (including the cathode and anode, electrolyte volume, composition, and concentration), the measurements (including charge/discharge techniques, rates, DoC, DoD) and the specific calculation equations (including voltage, capacity, energy density, power density, self-discharge, etc.) on how these parameters are determined. It is a matter of utmost urgency for the Mn-based battery community to establish widely accepted guidelines for standardizing calculations and measurements. In addition, the Mn-based batteries with extraordinary electrochemical performance and multi-functions such as the demonstrated ultralow temperature operation of the MnO_2-hydronium battery,[153] flexible and wearable devices, and self-charging properties are exciting directions to be explored for unique applications.

6.3. Simulation and Theoretical Calculation

In combination with experimental observations by advanced characterization tools, ab initio kinetic simulation, theoretical calculations, as well as machine learning are powerful tools to gain fundamental insights into the principles of the Mn-based batteries with the Mn^{2+}/MnO_2 chemistry. For example, the ab initio kinetic simulation of the Mn-based batteries can provide detailed information about behaviors of the redox reactions on a molecular level. Numerical simulations such as the finite element method can assist in failure analysis and lifespan prediction of the batteries.[168,169] In addition, the first-principle calculations can be used to predict the battery redox reactions at an atomic level.[170] Through the DFT calculation of the adsorption energies of the intermediates, we can analyze the electrode surface species and the preferred reaction pathways in specific electrolytes, thus gain a comprehensive insight into the energy storage mechanism.[171] Furthermore, artificial intelligence and machine learning will play invaluable roles in the prediction and refinement of the most rational materials combinations, cell manufacturing, and operation.[172]

6.4. New Mn-Based Battery Chemistry

Despite the recent progress in the development of Mn-based batteries with the Mn^{2+}/MnO_2 mechanism, there remain some critical challenges that require further investigations, and therefore call for the development of new Mn-based battery chemistry with enhanced performance. The cathode Mn^{2+}/MnO_2 reactions with two-electron charge transfer give rise to theoretical capacity of ≈616 mAh g^{-1} based on the deposited MnO_2 solely. However, the pursuit of the cathode reactions with multiple (>2) electrons transfers and superior output voltage is attractive yet very challenging. A recent study implies that the Mn^{2+}/MnO_4^- reactions may be reversible in a Mn-based battery with acidic MnO_4^- in the cathode electrolyte.[150] However, more effort should be devoted to the development of new Mn cathode with superior performance. On the other hand, the matching anodes of the Mn-based batteries, which are generally metallic materials, have potential risks of HER and dendrite formation. As HER accelerates on the metal anode in acidic electrolytes, while the cathode Mn^{2+}/MnO_2 reactions perform well with a certain acidity, it is important to optimize the acidity of the

electrolyte for both the cathode and anode reactions to maximize the overall electrochemical performance. Meanwhile, the dendrite formation due to uneven and irregular metal plating is critical to the cycling stability and safety of the battery. In this regard, the employment of non-metals such as polymers,[153] carbon materials[82] and other materials as alternative anodes provides additional opportunities to enrich the Mn-based battery chemistry. Exploring new cathodes and anodes with proper functionalities will contribute to the development of new Mn-based battery chemistry.

6.5. Battery System Integration

The battery system integration refers to the overall considerations of Mn-based battery as a delicate system from various aspects with respect to battery key components (current collector, cathode, anode, separator, electrolyte, as well as, cell configuration, packing, and manufacturing), cost, performance, and real-life applications in order to maximize the techno-economic benefits. As the capacity of both cathode and anode are expected to increase, their current collectors are required to have improved mass loadings for active materials, which is a challenge to the current state-of-the-art Mn-based batteries. Future strategy will be focused on exploring current collectors with lightweight, high surface area, good electrical conductivity, and hydrophilicity. The adoption of cathode, anode, and electrolyte needs to be considered simultaneously to comply with the standard guidelines for the electrochemical performance, while maintaining low cost for practical applications. Special attention needs to be paid to the optimization of the Mn^{2+}, H^{+}, and other cations/anions in the electrolyte, so as to understand their incorporated impacts on the electrochemical performance in terms of discharge voltage, capacity, charge/discharge rates, long-term stability, and self-discharge. In addition, the cost of Mn-based battery should be evaluated when relatively expensive separators/ion-exchange-membranes are applied to the battery. Overall, the system-level concerns and solutions in the development of Mn-based batteries will help translate the research lab-based battery designs to the industry with scalable production in a cost-effective manner.[37]

6.6. Scale-Up and Commercialization

Aqueous Mn-based batteries with the cathode Mn^{2+}/MnO_2 chemistry have shown the advantages of low-cost, high-level safety, environmental-friendliness, good electrochemical performance, and long-term stability, representing promising candidates for future large-scale energy storage applications. By integration with the electric grid, the Mn-based batteries can make up for the randomness and intermittence of the renewable energy sources, hence effectively improve the performance of the power grid.[173] Low cost, scalable manufacturing, and long-term shelf life are among the most prominent challenges that need to be overcome for the Mn-based batteries toward large-scale energy storage applications. Despite the recent developments where lab-scale prototype batteries have shown very attractive features, the Mn-based batteries remain challenging for large-scale commercialization.[151] We believe that the gradual shift from the lab research to industry, and the further development of the Mn-based batteries in the industry with standard guidelines and targeted applications will enable commercially viable projects to fulfill the practical energy storage solutions.

Acknowledgements

W.C. acknowledges the startup funds from University of Science and Technology of China (KY2060000150) and the support from USTC Center for Micro and Nanoscale Research and Fabrication. H.N.A. and Y.C. would like to acknowledge the support of King Abdullah University of Science and Technology (KAUST) for their fund under grant # OSR-CRG2018-3735.

Conflict of Interest

The authors declare no conflict of interest.

Keywords

aqueous batteries, deposition and stripping chemistry, large-scale energy storage, manganese batteries

Received: September 11, 2020
Revised: October 17, 2020
Published online: December 21, 2020

[1] C. McGlade, P. Ekins, *Nature* **2015**, *517*, 187.
[2] R. F. Service, *Science* **2018**, *362*, 508.
[3] S. Chu, A. Majumdar, *Nature* **2012**, *488*, 294.
[4] N. Abas, A. Kalair, N. Khan, *Futures* **2015**, *69*, 31.
[5] B. Dunn, H. Kamath, J.-M. Tarascon, *Science* **2011**, *334*, 928.
[6] J. G. B. Derraik, *Mar. Pollut. Bull.* **2002**, *44*, 842.
[7] B. Obama, *Science* **2017**, *355*, 126.
[8] Z. Zhang, C. Shi, G. Xiao, L. Kai, J. Yue, *Ceram. Int.* **2017**, *43*, 10052.
[9] H. Li, L. Ma, C. Han, Z. Wang, Z. Liu, Z. Tang, C. Zhi, *Nano Energy* **2019**, *62*, 550.
[10] S. Chu, Y. Cui, N. Liu, *Nat. Mater.* **2016**, *16*, 16.
[11] H. J. Herfurth, *Nature* **2008**, *451*, 652.
[12] S. Liu, Y. Zhu, J. Xie, Y. Huo, H. Y. Yang, T. Zhu, G. Cao, X. Zhao, S. Zhang, *Adv. Energy Mater.* **2014**, *4*, 1301960.
[13] B. Tang, L. Shan, S. Liang, J. Zhou, *Energy Environ. Sci.* **2019**, *12*, 3288.
[14] J. Rugolo, M. Aziz, *Energy Environ. Sci.* **2012**, *5*, 7151.
[15] Y. Wu, M. Wang, Y. Tao, K. Zhang, M. Cai, Y. Ding, X. Liu, T. Hayat, A. Alsaedi, S. Dai, *Adv. Funct. Mater.* **2020**, *30*, 1907120.
[16] K. Wang, K. Jiang, B. Chung, T. Ouchi, P. J. Burke, D. A. Boysen, D. J. Bradwell, H. Kim, U. Muecke, D. R. Sadoway, *Nature* **2014**, *514*, 348.
[17] P. Gu, M. Zheng, Q. Zhao, X. Xiao, H. Xue, H. Pang, *J. Mater. Chem. A* **2017**, *5*, 7651.
[18] Y. Hu, T. Zhang, F. Cheng, Q. Zhao, X. Han, J. Chen, *Angew. Chem., Int. Ed.* **2015**, *54*, 4338.
[19] J. Y. Hwang, S.-T. Myung, Y.-K. Sun, *Chem. Soc. Rev.* **2017**, *46*, 3529.
[20] A. Yoshino, *Angew. Chem., Int. Ed.* **2012**, *51*, 5798.
[21] H. Kim, J. Hong, K.-Y. Park, H. Kim, S.-W. Kim, K. Kang, *Chem. Rev.* **2014**, *114*, 11788.
[22] K. Cao, H. Liu, X. Chang, Y. Li, Y. Wang, L. Jiao, *Adv. Mater. Technol.* **2017**, *2*, 1600221.

[23] J. Hu, Y. Xiao, H. Tang, H. Wang, Z. Wang, C. Liu, H. Zeng, Q. Huang, Y. Ren, C. Wang, W. Zhang, F. Pan, *Nano Lett.* **2017**, *17*, 4934.
[24] S. Sun, H. Miao, Y. Xue, Q. Wang, Q. Zhang, Z. Dong, S. Li, H. Huang, Z. Liu, *J. Electrochem. Soc.* **2017**, *164*, F768.
[25] Y. Yang, G. Zheng, Y. Cui, *Energy Environ. Sci.* **2013**, *6*, 1552.
[26] L. Li, A.-R. O. Raji, J. M. Tour, *Adv. Mater.* **2013**, *25*, 6298.
[27] F. Wang, O. Borodin, M. S. Ding, M. Gobet, J. Vatamanu, X. Fan, T. Gao, N. Edison, Y. Liang, W. Sun, *Joule* **2018**, *2*, 927.
[28] J. Zhang, Y. Shi, Y. Ding, W. Zhang, G. Yu, *Nano Lett.* **2016**, *16*, 7276.
[29] W. Mao, G. Ai, Y. Dai, Y. Fu, Y. Ma, S. Shi, R. Soe, X. Zhang, D. Qu, Z. Tang, V. S. Battaglia, *J. Power Sources* **2016**, *310*, 54.
[30] J. M. Tarascon, M. Armand, *Nature* **2001**, *414*, 359.
[31] H. Ao, Y. Zhao, J. Zhou, W. Cai, X. Zhang, Y. Zhu, Y. Qian, *J. Mater. Chem. A* **2019**, *7*, 18708.
[32] M. Song, H. Tan, D. Chao, H. J. Fan, *Adv. Funct. Mater.* **2018**, *28*, 1802564.
[33] A. Konarov, N. Voronina, J. H. Jo, Z. Bakenov, Y.-K. Sun, S.-T. Myung, *ACS Energy Lett.* **2018**, *3*, 2620.
[34] N. Alias, A. A. Mohamad, *J. Power Sources* **2015**, *274*, 237.
[35] T. Liu, X. Cheng, H. Yu, H. Zhu, N. Peng, R. Zheng, J. Zhang, M. Shui, Y. Cui, J. Shu, *Energy Storage Mater.* **2019**, *18*, 68.
[36] C. Wessells, R. A. Huggins, Y. Cui, *J. Power Sources* **2011**, *196*, 2884.
[37] D. Chao, W. Zhou, F. Xie, C. Ye, H. Li, M. Jaroniec, S.-Z. Qiao, *Sci. Adv.* **2020**, *6*, eaba4098.
[38] S. Lian, C. Sun, W. Xu, W. Huo, Y. Luo, K. Zhao, G. Yao, W. Xu, Y. Zhang, Z. Li, K. Yu, H. Zhao, H. Cheng, J. Zhang, L. Mai, *Nano Energy* **2019**, *62*, 79.
[39] C. Guo, Q. Zhou, H. Liu, S. Tian, B. Chen, J. Zhao, J. Li, *Electrochim. Acta* **2019**, *324*, 134867.
[40] X. Fan, K. Ni, J. Han, S. Wang, L. Gou, D.-L. Li, *Funct. Mater. Lett.* **2019**, *12*, 1950073.
[41] E. Iruin, A. R. Mainar, M. Enterria, N. Ortiz-Vitoriano, J. A. Blazquez, L. C. Colmenares, T. Rojo, S. Clark, B. Horstmann, *Electrochim. Acta* **2019**, *320*, 134557.
[42] S. Khamsanga, R. Pornprasertsuk, T. Yonezawa, A. A. Mohamad, S. Kheawhom, *Sci. Rep.* **2019**, *9*, 8441.
[43] H. Zhao, J. Xu, D. Yin, Y. Du, *Chem. - Eur. J.* **2018**, *24*, 18220.
[44] Y. Tang, S. Zheng, Y. Xu, X. Xiao, H. Xue, H. Pang, *Energy Storage Mater.* **2018**, *12*, 284.
[45] Y. Zhang, C. Yuan, K. Ye, X. Jiang, J. Yin, G. Wang, D. Cao, *Electrochim. Acta* **2014**, *148*, 237.
[46] B. Li, J. Chai, X. Ge, T. An, P. C. Lim, Z. Liu, Y. Zong, *Chemnanomat* **2017**, *3*, 401.
[47] Y. Wang, W. Huo, X. Yuan, Y. Zhang, *Acta Phys.-Chim. Sin.* **2020**, *36*, 1904007.
[48] C. Wei, C. Xu, B. Li, H. Du, F. Kang, *J. Phys. Chem. Solids* **2012**, *73*, 1487.
[49] B. Lee, H. R. Lee, H. Kim, K. Y. Chung, B. W. Cho, H. O. Si, *Chem. Commun.* **2015**, *51*, 9265.
[50] Y. Zhang, S. Deng, M. Luo, G. Pan, Y. Zeng, X. Lu, C. Ai, Q. Liu, Q. Xiong, X. Wang, X. Xia, J. Tu, *Small* **2019**, *15*, 1905452.
[51] C. Xie, T. Li, C. Deng, Y. Song, H. Zhang, X. Li, *Energy Environ. Sci.* **2020**, *13*, 135.
[52] C. Ling, R. Zhang, T. S. Arthur, F. Mizuno, *Chem. Mater.* **2015**, *27*, 5799.
[53] K. Zhang, X. Han, Z. Hu, X. Zhang, Z. Tao, J. Chen, *Chem. Soc. Rev.* **2015**, *44*, 699.
[54] W. Wei, X. Cui, W. Chen, D. G. Ivey, *Chem. Soc. Rev.* **2011**, *40*, 1697.
[55] D.-S. Li, Q.-L. Gao, H. Zhang, Y.-F. Wang, W.-L. Liu, M.-M. Ren, F.-G. Kong, S.-J. Wang, J. Chang, *Appl. Surf. Sci.* **2020**, *510*, 145458.
[56] D. Aurbach, Z. Lu, A. Schechter, Y. Gofer, E. Levi, *Nature* **2000**, *407*, 724.
[57] Y. Liu, X. Chi, Q. Han, Y. Du, J. Huang, Y. Liu, J. Yang, *J. Power Sources* **2019**, *443*, 227244.
[58] G. Wang, L. Zhang, J. Zhang, *Chem. Soc. Rev.* **2012**, *41*, 791.
[59] M. Huang, M. Li, C. Niu, Q. Li, L. Mai, *Adv. Funct. Mater.* **2019**, *29*, 1807847.
[60] S. Hassan, M. Suzuki, A. A. El-Moneim, *J. Power Sources* **2014**, *246*, 68.
[61] B. Lee, S. Y. Chong, H. R. Lee, K. Y. Chung, H. O. Si, *Sci. Rep.* **2015**, *4*, 6066.
[62] J. Mcbreen, *Electrochim. Acta* **1975**, *20*, 221.
[63] F. Shi, C. Mang, H. Liu, Y. Dong, *New J. Chem.* **2020**, *44*, 653.
[64] C. Wang, Y. Zeng, X. Xiao, S. Wu, G. Zhong, K. Xu, Z. Wei, W. Su, X. Lu, *J. Energy Chem.* **2020**, *43*, 182.
[65] M. Rana, V. S. Avvaru, N. Boaretto, V. A. de la Pena O'Shea, R. Marcilla, V. Etacheri, J. J. Vilatela, *J. Mater. Chem. A* **2019**, *7*, 26596.
[66] H. Zhang, D. Cao, X. Bai, *J. Power Sources* **2019**, *444*, 227299.
[67] C. Yuan, Y. Zhang, Y. Pan, X. Liu, G. Wang, D. Cao, *Electrochim. Acta* **2014**, *116*, 404.
[68] X. Liu, J. Yi, K. Wu, Y. Jiang, Y. Liu, B. Zhao, W. Li, J. Zhang, *Nanotechnology* **2020**, *31*, 122001.
[69] D. Wang, L. Wang, G. Liang, H. Li, Z. Liu, Z. Tang, J. Liang, C. Zhi, *ACS Nano* **2019**, *13*, 10643.
[70] A. R. Armstrong, P. G. Bruce, *Nature* **1996**, *381*, 499.
[71] C. Guo, H. Liu, J. Li, Z. Hou, J. Liang, J. Zhou, Y. Zhu, Y. Qian, *Electrochim. Acta* **2019**, *304*, 370.
[72] Y. Jiang, D. Ba, Y. Li, J. Liu, *Adv. Sci.* **2020**, *7*, 190295.
[73] M. Salehi, Z. Shariatinia, *Electrochim. Acta* **2016**, *188*, 428.
[74] X. Wu, A. Markir, Y. Xu, C. Zhang, D. P. Leonard, W. Shin, X. Ji, *Adv. Funct. Mater.* **2019**, *29*, 1900911.
[75] L. Chen, Z. Yang, F. Cui, J. Meng, Y. Jiang, J. Long, X. Zeng, *Mater. Chem. Front.* **2020**, *4*, 213.
[76] W. Chen, G. Li, A. Pei, Y. Li, L. Liao, H. Wang, J. Wan, Z. Liang, G. Chen, H. Zhang, J. Wang, Y. Cui, *Nat. Energy* **2018**, *3*, 428.
[77] C. Liu, X. Chi, Q. Han, Y. Liu, *Adv. Energy Mater.* **2020**, *10*, 1903589.
[78] G. Li, W. Chen, H. Zhang, Y. Gong, F. Shi, J. Wang, R. Zhang, G. Chen, Y. Jin, T. Wu, Z. Tang, Y. Cui, *Adv. Energy Mater.* **2020**, *10*, 1902085.
[79] D. Chao, W. Zhou, C. Ye, Q. Zhang, Y. Chen, L. Gu, K. Davey, S.-Z. Qiao, *Angew. Chem., Int. Ed.* **2019**, *58*, 7823.
[80] J. Huang, Z. Guo, X. Dong, D. Bin, Y. Wang, Y. Xia, *Sci. Bull.* **2019**, *64*, 1780.
[81] L. Wei, L. Zeng, M. C. Wu, H. R. Jiang, T. S. Zhao, *J. Power Sources* **2019**, *423*, 203.
[82] Y. Feng, Q. Zhang, S. Liu, J. Liu, Z. Tao, J. Chen, *J. Mater. Chem. A* **2019**, *7*, 2922.
[83] J. Huang, L. Yan, D. Bin, X. Dong, Y. Wang, Y. Xia, *J. Mater. Chem. A* **2020**, *8*, 5959.
[84] G. Fang, J. Zhou, A. Pan, S. Liang, *ACS Energy Lett.* **2018**, *3*, 2480.
[85] Z. Ma, T. Zhao, *Electrochim. Acta* **2016**, *201*, 165.
[86] G. Liang, F. Mo, Q. Yang, Z. Huang, X. Li, D. Wang, Z. Liu, H. Li, Q. Zhang, C. Zhi, *Adv. Mater.* **2019**, *31*, 1905873.
[87] Y. H. Lu, J. B. Goodenough, Y. Kim, *J. Am. Chem. Soc.* **2011**, *133*, 5756.
[88] A. M. Kannan, S. Bhavaraju, F. Prado, M. M. Raja, A. Manthirama, *J. Electrochem. Soc.* **2002**, *149*, A483.
[89] C. Xu, B. Li, H. Du, F. Kang, *Angew. Chem., Int. Ed.* **2012**, *51*, 933.
[90] A. Era, Z. Takehara, S. Yoshizawa, *Electrochim. Acta* **1967**, *12*, 1199.
[91] F. R. McLarnon, E. J. Cairns, *J. Electrochem. Soc.* **1991**, *138*, 645.
[92] B. J. Hertzberg, A. Huang, A. Hsieh, M. Chamoun, G. Davies, J. K. Seo, Z. Zhong, M. Croft, C. Erdonmez, Y. S. Meng, *Chem. Mater.* **2016**, *28*, 4536.
[93] V. K. Nartey, L. Binder, A. Huber, *J. Power Sources* **2000**, *87*, 205.
[94] S. V. Ovsyannikov, A. M. Abakumov, A. A. Tsirlin, W. Schnelle, R. Egoavil, J. Verbeeck, G. V. Tendeloo, K. V. Glazyrin, *Angew. Chem., Int. Ed.* **2013**, *125*, 1534.
[95] J. W. Gallaway, M. Menard, B. Hertzberg, Z. Zhong, M. Croft, L. A. Sviridov, *J. Electrochem. Soc.* **2015**, *A162*, A162.

[96] J. F. Parker, C. N. Chervin, E. S. Nelson, D. R. Rolison, J. W. Long, *Energy Environ. Sci.* **2014**, *7*, 1117.
[97] Y. Shen, K. Kordesch, *J. Power Sources* **2000**, *87*, 162.
[98] E. Moazzen, E. V. Timofeeva, J. A. Kaduk, C. U. Segre, *Cryst. Growth Des.* **2019**, *19*, 1584.
[99] M. Minakshi, P. Singh, M. Carter, K. Prince, *Electrochem. Solid Lett.* **2008**, *11*, 515.
[100] M. Manickam, P. Singh, T. B. Issa, S. Thurgate, R. D. Marco, *J. Power Sources* **2004**, *138*, 319.
[101] X. Zhu, X. Wu, T. N. L. Doan, Y. Tian, H. Zhao, P. Chen, *J. Power Sources* **2016**, *326*, 498.
[102] C. Guo, J. Li, Y. Chu, H. Li, H. Zhang, L. Hou, Y. Wei, J. Liu, S. Xiong, *Dalton Trans.* **2019**, *48*, 7403.
[103] J. Yang, J. Wang, L. Zhu, Q. Gao, W. Zeng, J. Wang, Y. Li, *Ceram. Int.* **2018**, *44*, 23073.
[104] K. Zhao, C. Sun, Y. Yu, Y. Dong, C. Zhang, C. Wang, P. M. Voyles, L. Mai, X. Wang, *ACS Appl. Mater. Interfaces* **2018**, *10*, 44376.
[105] G. G. Yadav, J. W. Gallaway, D. E. Turney, M. Nyce, J. Huang, X. Wei, S. Banerjee, *Nat. Commun.* **2017**, *8*, 14424.
[106] C. Mondoloni, M. Laborde, J. Rioux, E. Andoni, C. Levyclement, *J. Electrochem. Soc.* **1992**, *139*, 954.
[107] B. Hertzberg, L. Sviridov, E. A. Stach, T. Gupta, D. Steingart, *J. Electrochem. Soc.* **2014**, *161*, A835.
[108] N. D. Ingale, J. W. Gallaway, M. Nyce, A. Couzis, S. Banerjee, *J. Power Sources* **2015**, *276*, 7.
[109] L. Bat, D. Y. Qu, B. E. Conway, *J. Electrochem. Soc.* **1993**, *140*, 884.
[110] C. G. Castledine, B. E. Conway, *J. Appl. Electrochem.* **1995**, *25*, 707.
[111] M. H. Alfaruqi, J. Gim, S. Kim, J. Song, J. Jo, S. Kim, V. Mathew, J. Kim, *J. Power Sources* **2015**, *288*, 320.
[112] J. Lee, J. B. Ju, W. I. Cho, B. W. Cho, S. H. Oh, *Electrochim. Acta* **2013**, *112*, 138.
[113] H. Pan, Y. Shao, P. Yan, Y. Cheng, K. S. Han, Z. Nie, C. Wang, J. Yang, X. Li, P. Bhattacharya, K. T. Mueller, J. Liu, *Nat. Energy* **2016**, *1*, 16039.
[114] M. H. Alfaruqi, S. Islam, J. Gim, J. Song, S. Kim, D. T. Pham, J. Jo, Z. Xiu, V. Mathew, J. Kim, *Chem. Phys. Lett.* **2016**, *650*, 64.
[115] M. H. Alfaruqi, J. Gim, S. Kim, J. Song, D. T. Pham, J. Jo, Z. Xiu, V. Mathew, J. Kim, *Electrochem. Commun.* **2015**, *60*, 121.
[116] J. Huang, Z. Guo, Y. Ma, D. Bin, Y. Wang, Y. Xia, *Small Methods* **2019**, *3*, 1800272.
[117] T. Yamamoto, T. Shoji, *Cheminform* **1986**, *17*, 017.
[118] T. Shoji, M. Hishinuma, T. Yamamoto, *J. Appl. Electrochem.* **1988**, *18*, 521.
[119] D. Xu, B. Li, C. Wei, Y.-B. He, H. Du, X. Chu, X. Qin, Q.-H. Yang, F. Kang, *Electrochim. Acta* **2014**, *133*, 254.
[120] I. Stosevski, A. Bonakdarpour, F. Cuadra, D. P. Wilkinson, *Chem. Commun.* **2019**, *55*, 2082.
[121] N. Qiu, H. Chen, Z. Yang, S. Sun, Y. Wang, *Electrochim. Acta* **2018**, *272*, 154.
[122] J. Yang, J. Wang, S. Ma, B. Ke, L. Yu, W. Zeng, Y. Li, J. Wang, *Phys. E* **2019**, *109*, 191.
[123] D.-S. Li, S. Wu, Y.-F. Wang, M. Sun, W.-L. Liu, M.-M. Ren, F.-G. Kong, S.-J. Wang, X.-Q. Wang, *J. Nanopart. Res.* **2019**, *21*, 52.
[124] J. Mao, F.-F. Wu, W.-H. Shi, W.-X. Liu, X.-L. Xu, G.-F. Cai, Y.-W. Li, X.-H. Cao, *Chin. J. Polym. Sci.* **2020**, *38*, 514.
[125] Y. Li, S. Wang, J. R. Salvador, J. Wu, B. Liu, W. Yang, J. Yang, W. Zhang, J. Liu, J. Yang, *Chem. Mater.* **2019**, *31*, 2036.
[126] W. Sun, F. Wang, S. Hou, C. Yang, C. Wang, *J. Am. Chem. Soc.* **2017**, *139*, 9775.
[127] X. Gao, H. Wu, W. Li, Y. Tian, Y. Zhang, H. Wu, L. Yang, G. Zou, H. Hou, X. Ji, *Small* **2020**, *16*, 1905842.
[128] H. Wei, X. Hu, X. Zhang, Z. Yu, T. Zhou, Y. Liu, Y. Liu, Y. Wang, J. Xie, L. Sun, M. Liang, P. Jiang, *Energy Technol.* **2019**, *7*, 1800912.
[129] M. Chamoun, W. R. Brant, C.-W. Tai, G. Karlsson, D. Noréus, *Energy Storage Mater.* **2018**, *15*, 251.
[130] B. Wu, G. Zhang, M. Yan, T. Xiong, L. Mai, *Small* **2018**, *14*, 1703850.
[131] Q. Zhao, X. Chen, Z. Wang, L. Yang, R. Qin, J. Yang, Y. Song, S. Ding, M. Weng, W. Huang, J. Liu, W. Zhao, G. Qian, K. Yang, Y. Cui, H. Chen, F. Pan, *Small* **2019**, *15*, 1904545.
[132] N. Zhang, F. Cheng, J. Liu, L. Wang, X. Long, X. Liu, F. Li, J. Chen, *Nat. Commun.* **2017**, *8*, 405.
[133] N. Zhang, F. Cheng, Y. Liu, Q. Zhao, K. Lei, C. Chen, X. Liu, J. Chen, *J. Am. Chem. Soc.* **2016**, *138*, 12894.
[134] M. Li, Q. He, Z. Li, Q. Li, Y. Zhang, J. Meng, X. Liu, S. Li, B. Wu, L. Chen, Z. Liu, W. Luo, C. Han, L. Mai, *Adv. Energy Mater.* **2019**, *9*, 1901469.
[135] S. Wang, Q. Wang, W. Zeng, M. Wang, L. Ruan, Y. Ma, *Nano-Micro Lett.* **2019**, *11*, 70.
[136] Y. Huang, J. Mou, W. Liu, X. Wang, L. Dong, F. Kang, C. Xu, *Nano-Micro Lett.* **2019**, *11*, 49.
[137] M. P. Owen, G. A. Lawrance, S. W. Donne, *Electrochim. Acta* **2007**, *52*, 4630.
[138] M. Chotkowski, Z. Rogulski, A. Czerwiński, *J. Electroanal. Chem.* **2011**, *651*, 237.
[139] P. G. Perret, P. R. L. Malenfant, C. Bock, B. MacDougall, *J. Electrochem. Soc.* **2012**, *159*, A1554.
[140] A. J. Gibson, B. Johannessen, Y. Beyad, J. Allen, S. W. Donne, *J. Electrochem. Soc.* **2016**, *163*, H305.
[141] G. Liang, F. Mo, H. Li, Z. Tang, Z. Liu, D. Wang, Q. Yang, L. Ma, C. Zhi, *Adv. Energy Mater.* **2019**, *9*, 1901838.
[142] W. Chen, Y. Jin, J. Zhao, N. Liu, Y. Cui, *Proc. Natl. Acad. Sci. USA* **2018**, *115*, 11694.
[143] Z. Zhu, M. Wang, Y. Meng, Z. Lin, Y. Cui, W. Chen, *Nano Lett.* **2020**, *20*, 3278.
[144] J. Shin, J. K. Seo, R. Yaylian, A. Huang, Y. S. Meng, *Int. Mater. Rev.* **2019**, *65*, 356.
[145] Q. Li, X. Cui, Q. Pan, *ACS Appl. Mater. Interfaces* **2019**, *11*, 38762.
[146] N. Ma, P. Wu, Y. Wu, D. Jiang, G. Lei, *Funct. Mater. Lett.* **2019**, *12*, 1930003.
[147] D. Chao, C. Ye, F. Xie, W. Zhou, Q. Zhang, Q. Gu, K. Davey, L. Gu, S.-Z. Qiao, *Adv. Mater.* **2020**, *32*, 2001894.
[148] X. Guo, J. Zhou, C. Bai, X. Li, G. Fang, S. Liang, *Mater. Today Energy* **2020**, *16*, 100396.
[149] L. Wang, Q. Wu, A. Abraham, P. J. West, L. M. Housel, G. Singh, N. Sadique, C. D. Quilty, D. Wu, E. S. Takeuchi, A. C. Marschilok, K. J. Takeuchi, *J. Electrochem. Soc.* **2019**, *166*, A3575.
[150] G. G. Yadav, D. Turney, J. Huang, X. Wei, S. Banerjee, *ACS Energy Lett.* **2019**, *4*, 2144.
[151] C. Zhong, B. Liu, J. Ding, X. Liu, Y. Zhong, Y. Li, C. Sun, X. Han, Y. Deng, N. Zhao, W. Hu, *Nat. Energy* **2020**, *5*, 440.
[152] S. He, J. Wang, X. Zhang, J. Chen, Z. Wang, T. Yang, Z. Liu, Y. Liang, B. Wang, S. Liu, L. Zhang, J. Huang, J. Huang, L. A. O'Dell, H. Yu, *Adv. Energy Mater.* **2019**, *29*, 1905228.
[153] Z. Guo, J. Huang, X. Dong, Y. Xia, L. Yan, Z. Wang, Y. Wang, *Nat. Commun.* **2020**, *11*, 959.
[154] J. Wang, X. Sun, H. Zhao, L. Xu, J. Xia, M. Luo, Y. Yang, Y. Du, *J. Phys. Chem. C* **2019**, *123*, 22735.
[155] M. Liu, Q. Zhao, H. Liu, J. Yang, X. Chen, L. Yang, Y. Cui, W. Huang, W. Zhao, A. Song, Y. Wang, S. Ding, Y. Song, G. Qian, H. Chen, F. Pan, *Nano Energy* **2019**, *64*, 103942.
[156] S. Zhang, W. Guo, F. Yang, P. Zheng, R. Qiao, Z. Li, *Batteries Supercaps* **2019**, *2*, 627.
[157] G. L. Soloveichik, *Chem. Rev.* **2015**, *115*, 11533.
[158] C. J. Clarke, G. J. Browning, S. W. Donne, *Electrochim. Acta* **2006**, *51*, 5773.
[159] M. F. Dupont, S. W. Donne, *Electrochim. Acta* **2016**, *191*, 479.
[160] M. F. Dupont, S. W. Donne, *Electrochim. Acta* **2014**, *120*, 219.
[161] S. W. Donne, F. H. Feddrix, R. Glockner, S. Marion, T. Norby, *Solid State Ionics* **2002**, *152-153*, 695.
[162] G. J. Browning, S. W. Donne, *J. Appl. Electrochem.* **2005**, *35*, 437.

[163] S. Hameer, J. L. Van Niekerk, *Int. J. Energy Res.* **2015**, *39*, 1179.
[164] C. Zhan, Z. Yao, J. Lu, L. Ma, V. A. Maroni, L. Li, E. Lee, E. E. Alp, T. Wu, J. Wen, Y. Ren, C. Johnson, M. M. Thackeray, M. K. Y. Chan, C. Wolverton, K. Amine, *Nat. Energy* **2017**, *2*, 963.
[165] A. M. Simes, A. C. Bastos, M. G. Ferreira, Y. González-García, S. González, R. M. Souto, *Corros. Sci.* **2007**, *49*, 726.
[166] A. D. Handoko, F. Wei, Jenndy, B. S. Yeo, Z. W. Seh, *Nat. Catal.* **2018**, *1*, 922.
[167] D. Liu, Z. Shadike, R. Lin, K. Qian, H. Li, K. Li, S. Wang, Q. Yu, M. Liu, S. Ganapathy, X. Qin, Q.-H. Yang, M. Wagemaker, F. Kang, X.-Q. Yang, B. Li, *Adv. Mater.* **2019**, *31*, 1806620.
[168] K. Jang, K. Joo, K. Kim, *Nanosci. Nanotechnol. Lett.* **2017**, *9*, 1165.
[169] J.-S. Park, J. H. Jo, Y. Aniskevich, A. Bakavets, G. Ragoisha, E. Streltsov, J. Kim, S.-T. Myung, *Chem. Mater.* **2018**, *30*, 6777.
[170] M. H. Alfaruqi, S. Islam, J. Lee, J. Jo, V. Mathew, J. Kim, *J. Mater. Chem. A* **2019**, *7*, 26966.
[171] Y. Y. Birdja, E. Perez-Gallent, M. C. Figueiredo, A. J. Gottle, F. Calle-Vallejo, M. T. M. Koper, *Nat. Energy* **2019**, *4*, 732.
[172] P. M. Attia, A. Grover, N. Jin, K. A. Severson, T. M. Markov, Y.-H. Liao, M. H. Chen, B. Cheong, N. Perkins, Z. Yang, P. K. Herring, M. Aykol, S. J. Harris, R. D. Braatz, S. Ermon, W. C. Chueh, *Nature* **2020**, *578*, 397.
[173] B. Li, M. Gu, Z. Nie, Y. Shao, Q. Luo, X. Wei, X. Li, J. Xiao, C. Wang, V. Sprenkle, W. Wang, *Nano Lett.* **2013**, *13*, 1330.
[174] A. Kozawa, R. A. Powers, *J. Electrochem. Soc.* **1966**, *113*, 830.
[175] J. K. Seo, J. Shin, H. Chung, P. Y. Meng, X. Wang, Y. S. Meng, *J. Phys. Chem. C* **2018**, *122*, 11177.
[176] F. Y. Cheng, J. Chen, X. L. Gou, P. W. Shen, *Adv. Mater.* **2005**, *17*, 2753.
[177] Q. Wang, J. Pan, Y. Sun, Z. Wang, *J. Power Sources* **2012**, *199*, 355.
[178] G. G. Yadav, X. Wei, J. Huang, J. W. Gallaway, D. E. Turney, M. Nyce, J. Secor, S. Banerjee, *J. Mater. Chem. A* **2017**, *5*, 15845.
[179] G. G. Yadav, J. Cho, D. Turney, B. Hawkins, X. Wei, J. Huang, S. Banerjee, M. Nyce, *Adv. Energy Mater.* **2019**, *9*, 1902270.
[180] J. Huang, Z. Wang, M. Hou, X. Dong, Y. Liu, Y. Wang, Y. Xia, *Nat. Commun.* **2018**, *9*, 2906.

Mingming Wang is a master student in the department of chemistry of the University of Science and Technology of China (USTC). He received his B.S. in Chemistry in 2019 from Anhui Normal University. Since then he has been a graduate student under the supervision of Prof. Wei Chen at USTC. His research interests focus on the aqueous batteries for large-scale energy storage application.

Xinhua Zheng is a Ph.D. candidate in the department of applied chemistry of the University of Science and Technology of China (USTC). He obtained his B.S. degree from Henan University of Technology in 2016 and his M.S. degree from Beijing Institute of Petrochemical Technology in 2019. He is currently under the supervision of Prof. Wei Chen at USTC. His research focuses on aqueous rechargeable batteries.

Yi Cui is a Professor in the Department of Materials Science and Engineering at Stanford University and SLAC National Accelerator Laboratory. He received his B.S. from the University of Science and Technology of China (USTC) in 1998 and his Ph.D. from Harvard University in 2002. He was a Miller Postdoctoral Fellow at University of California, Berkeley and joined in Stanford as a faculty member in 2005. His current research is on nanomaterials for energy and environment. He has founded four companies to commercialize technologies from his lab: Amprius, 4C Air, EEnotech, and EnerVenue.

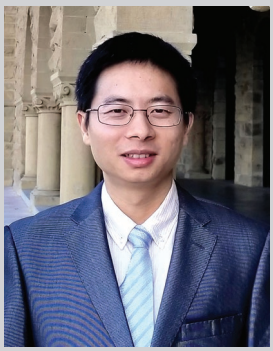

Wei Chen is a Professor in the department of applied chemistry of the USTC and the Hefei National Laboratory for Physical Sciences at the Microscale. He obtained his B.S. degree in materials physics from USTB in 2008 and his Ph.D. degree in materials science and engineering from KAUST in 2013. He then worked as a postdoc at Stanford University under the supervision of Prof. Yi Cui in 2014 and joined EEnotech in 2018 as a scientist before joining in USTC in 2019. His research interests involve advanced materials and technologies for energy storage and catalysis.